U. S. DEPARMENT OF COMMERCE
NATIONAL OCEANIC AND ATMOSPHERIC ADMINISTRATION
NATIONAL WEATHER SERVICE
NATIONAL METEOROLOGICAL CENTER

OFFICE NOTE 409

IMPLEMENTING A MASS FLUX CONVECTION PARAMETERIZATION PACKAGE FOR THE NMC MEDIUM-RANGE FORECAST MODEL

HUA-LU PAN
DEVELOPMENT DIVISION

WAN-SHU WU
GENERAL SCIENCES CORPORATION

SEPTEMBER 1995

ABSTRACT

On 11 August, 1993, a new convection parameterization package has become operational for the National Meteorological Center (NMC) Medium-Range Forecast (MRF) model replacing a Kuo (1965, 1974) scheme that has been in operation for over ten years. The new scheme is a version of a simplified Arakawa-Schubert (1974) scheme that uses the mass flux concept to adjust the atmospheric temperature and moisture field. The new scheme uses quasi-equilibrium assumption as a closure and includes a downdraft scheme that is analogous to the updraft scheme. Testing of the new scheme in parallel during Northern Hemisphere Spring shows a consistent improvement in the precipitation forecast verified against the observations taken by the high density North America rain gauge network maintained by the National Weather Service. Improvement in the tropical climatology and the tropical cyclone prediction have also been noted.

1. Introduction

The parameterization of sub-grid scale cumulus convection in a numerical weather prediction (NWP) model is a very difficult problem. Early NWP models had very coarse resolutions and sometimes became unstable numerically to actually "blow-up", especially when trying to simulate tropical storms. The inclusion of cumulus parameterization was intended to simulate the Conditional Instability of the Second Kind (CISK, Charney and Eliassen, 1964) and to prevent the forecast from blowing up. We now know that modern day numerical models with a reasonable resolution (e.g. 2° latitude by 2° longitude) can run without a cumulus parameterization package without numerical difficulties. The large scale condensation algorithm in most NWP models is capable of removing the super-saturation that occurs in the model and converts the excess water to precipitation and the release of latent heat. The problem is that the latent heat is released locally (in the vertical) and usually in the lower troposphere. This leads to the generation of many shallow vortices over the tropical ocean and distortion of the tropical general circulation. It is clear that cumulus convection, while a phenomenon that occurs on a spatial scale of 1-50 km, affects the large scale circulation by warming and drying the atmosphere over a deep layer . In order to maintain realistic vertical structure of the model temperature and moisture fields in our forecasts, a good cumulus parameterization is necessary. The effect of the deep cumulus is important not only for tropical synoptic scale systems but also for the maintenance of the atmospheric general circulation making it important to NWP models as well as General Circulation Models (GCMs).

At the National Meteorological Center (NMC), a Kuo parameterization scheme (Kuo, 1965, 1974) has been employed in the Medium-Range Forecast (MRF, Sela, 1980; Kanamitsu *et. al.*, 1991) model almost since the start of operation of the MRF. Over the years, many attempts have been made to improve the performance of the Kuo scheme which is simple and efficiently coded so that very little computer resource is required. While we like the computing efficiency of the Kuo scheme very much, we were unable to make real improvement of the scheme precisely because of the simplicity of the scheme. Among the problems that we have witnessed over the years are:

1) The model has a tendency to produce heavy precipitation centers near elevated land surfaces (e.g. the Andes, the Himalayas, and the east Africa highlands). While there is doubtlessly situations when there should be precipitation over these region, the model tends to produce rain daily without breaks given the slightest favorable condition. Over the Andes, this also reduces precipitation over the Amazon region, another undesirable side effect.

2) The model generates real and spurious tropical disturbances over the tropical oceanic regions. While the precipitation pattern over the tropical ocean may look reasonable in the first 12-24 hour forecast, the later forecasts will invariably show precipitation clustered into preferred centers with little precipitation outside these centers. The precipitation centers are usually quasi-stationary even when the tropical easterly waves that initiate them have moved away.

3) In extended range model runs, there is a severe deficiency of tropical precipitation over the warm oceanic regions. In model runs of 1-3 months, the resulting monthly mean precipitation pattern shows a lack of precipitation over the warmest tropical oceanic regions. When coupled with a global oceanic circulation model, the response of the model to sea surface temperature (SST) changes becomes much smaller because of this problem. This is a crucial problem for seasonal forecasts using coupled models.

4) The MRF model often fails to predict correctly convective precipitation region over North America during the convective season. Especially during northern hemispheric Spring and Summer, the large scale synoptic forcing over the U.S. are often weak and the model has a very difficult time forecasting the locations of convective precipitation.

For these reasons and many other related diagnoses made over the years, we have been dissatisfied with the Kuo scheme for some time. It is, however, very difficult to change to a totally different parameterization scheme. The MRF model is used in the Global Data Assimilation System (GDAS) to create the first-guess atmospheric state for the analysis system. This requires that the spin-up/spin-down character of the model be examined when a new convection scheme is considered. The model is also used to make the twice-daily Aviation forecast that goes out to 72 hours for aviation route forecast as well as short-range regional forecasts. Regional precipitation forecasts must be compared to the regional models such as the Nested Grid Model (NGM, Phillips, 1979) and the Eta model (Messinger *et al*, 1988). In addition, the National Hurricane Center has, in recent years, placed more emphasis on the Aviation forecast as one of the guidance for hurricane track forecast. Convection changes will certainly modify the prediction of hurricane tracks. In the 3-5 day and the 5-10 day medium-range and extended range forecast, it is hoped that a better convection scheme will improve the planetary scale wave forecast in these time ranges. As discussed in the previous paragraph, the monthly global precipitation prediction over the tropical ocean is of importance to the coupled model simulation of the response to SST anomalies. Finally, the Climate Analysis Center is interested in the general circulation behavior of the MRF model in aiding their understanding of inter-annual variations of the atmosphere. A new convection scheme may affect the monsoon simulation in ways beyond what one can expect based on short and medium range forecast experiments.

In order to meet all the challenges outlined above, it became obvious that fine-tuning the Kuo scheme is not sufficient. Instead, we decided, two years ago, to look for a more physically based scheme that can be improved in the future by adding more complex processes. We see this approach as our only hope to produce reasonable response in all the time ranges of concern to us. For the dynamic model, the most important function of a cumulus parameterization is the correct placement of the heating and the drying due to convection spatially and temporally in the forecast. Both the Kuo scheme and the Betts and Miller scheme (Betts and Miller, 1986) prescribe reference profiles of temperature and moisture in a convective environment and adjust the model variables toward them. While these approaches have merits in their simplicity and, in the case of the Betts and Miller scheme, in the approach to observed climate in convectively active region, it seems obvious that there should be different profiles for different situations, making continuing improvement of these schemes difficult. Through observational studies (e.g. Yanai *et al*, 1973) and theoretical studies (mainly, Arakawa and Schubert, 1974, hereafter referred to as AS), on the other hand, we have come to understand that, while convective updrafts take place over a small region, it is the convection induced subsidence in the environment and the detrainment of convective cloud properties that causes the warming and drying of the atmosphere. As elegantly described in AS : *the latent heat released within the clouds does not directly warm the environment, but it maintains the buoyancy of the clouds...The drying and warming of the environment, by the cumulus induced subsidence, are the indirect effects of condensation and release of latent heat.*, it is generally recognized that the parameterization scheme outlined in AS and implemented first by Lord (1978) is a more physically realistic approach to cumulus parameterization than the profile adjustment schemes. Furthermore, the framework outlined in AS can be improved as we gain further understanding of the cumulus convective complexes. The AS scheme is, however, complicated and requires the assumption of an ensemble of several cloud types at each grid point. The effect of rain-induced downdraft which has become recognized as an important component of a convective complex is also not included. While Cheng and Arakawa (1990) have started to address this aspect, the resulting scheme is even more complicated for operational implementation. A scheme that uses the idea of AS but simplified to only one cloud type was mentioned in Grell (1993) as responding favorably in his evaluation of cumulus parameterization schemes. We have adopted this scheme as the starting point of our effort to improve the parameterization of cumulus convection in the NMC MRF model.

In section 2, a brief description of the scheme is presented. Closure consideration is also discussed. Some of the tests that have been performed during the past two years will be presented in Section 3. Further discussion and conclusion are presented in Section 4.

2. A simple mass flux convection scheme

Since the basic physics of the scheme has been described in AS, Lord (1978), and Grell (1993), we will simply present the relevant equations without too much discussion. The scheme contains three basic parts: the static control, the dynamic control, and the feedback. In the static control, a simple cloud model is used to describe the thermodynamical properties of the mass (Eq. 1), the moist static energy (Eq. 2), and moisture (Eq. 3) within the updraft:

The mass flux (η) is normalized by the mass flux at the cloud base and can be modified by

$$\frac{\partial \eta}{\partial z} = \lambda_e - \lambda_d \tag{1}$$

$$\frac{\partial (\eta h_c)}{\partial z} = (\lambda_e \tilde{h} - \lambda_d h_c)\eta \tag{2}$$

$$\frac{\partial (\eta (q_c + l))}{\partial z} = \eta (\lambda_e \tilde{q} - \lambda_d (q_c + l) - r) \tag{3}$$

entrainment (λ_e) and detrainment (λ_d) as can moist static energy flux and moisture flux. The subscript c denotes the property of the cloud and the variables with a tilde that of the environment. The mixing ratio of water vapor (**q**) and the liquid water mixing ratio (**l**) constitute the moisture variable. For moisture flux, liquid water (**l**) detrainment and precipitation (**r**) also must be included. A similar equation set for downdraft exist and will be omitted for brevity.

Following Grell, we search for a parcel with a local maximum of moist static energy (**h**) in a model column as the starting point (SP) of the convection. The starting parcel is assumed to be below 700 hPa. The parcel is taken upward (conserving the saturation moist static energy) in search of a level of free convection (LFC). Once found, we re-derive the parcel mass flux assuming entrainment only from SP to LFC. Fifty percent of the mass is assumed to originate at SP. A specification of the percent of mass flux at the SP level allows us to determine the entrainment rate. Once LFC (our cloud base) is reached, the parcel is assumed to be non-entraining up to the cloud top - a point in the sounding where the parcel's saturation moist static energy becomes less than the moist static energy of the environment (i.e. loss of buoyancy). For the moisture budget, rain (**r**) is also parameterized. Again, we follow the original prescription of Lord in parameterization a portion of the condensed water (**l**) to rain (Ice-phase physics has been neglected in this version). All convective mass flux detrains at the cloud top.

A saturated downdraft is assumed as in Grell, but the downdraft detrains below LFC in such a manner that fifteen percent of the mass flux pass through the SP level, similar to the treatment of entrainment in the updraft. The downdraft starting level in Grell was set at the minimum moist static energy level. We found this to generate excessive cooling below cloud base. Following the observation work of Nitta (1975), we try to set the starting level near 400 hPa and select the level above the minimum moist static energy level. The fraction of downdraft mass flux to updraft mass flux is derived following Fritsch and Chappel (1980, hereafter referred to as FC) as was done in Grell. The formula in FC is the result of a curve-fit of the precipitation efficiency as a function of the vertical wind shear within the cloud.

The dynamic control is based on the quasi-equilibrium assumption of AS that the de-stabilization of an air column by the large scale atmosphere is nearly balanced by the stabilization of the cumulus. Assuming that the grid-averaged cloud work function varies slowly compared to the adjustment time scale of the cumulus, a closure of the parameterization scheme is obtained. The cloud work function is a measure of the buoyancy of the cloud and is defined as:

$$A_u = \int_{z_0}^{z_t} \frac{g}{C_p T(z)} \frac{\eta}{1+\gamma} [h(z) - \tilde{h}^*(z)] dz \tag{4}$$

where h is the moist static energy of the cloud, $\tilde{h}^*$ is the environmental saturation moist static energy and $\gamma = \frac{L}{C_p} (\frac{\partial \tilde{q}^*}{\partial T})_P$. For downdraft, a similar cloud work function (A_d) is defined and added to the updraft to form the total cloud work function A . The cloud work function at a new time step (after advection and turbulent mixing), A^+ ,and a reference cloud work function derived from observations by Lord, A^0, are used to provide an estimate of the large scale de-stabilization:

$$\frac{dA}{dt}\Big|_{ls} = \frac{A^{+} - A^{0}}{\Delta t} \tag{5}$$

where the subscript ls denotes the large scale contribution to the time rate of change of the cloud work function and Δt is an adjustment time scale presently set to one hour. One can calculate the warming and drying of the environment due to the presence of a cloud of unit mass flux (this is the feedback mechanism that will be described later) over a small time interval δt. The difference between the cloud work function of the adjusted sounding, A^{*}, and the cloud work function A^{+} provides the stabilization effect of the cumulus cloud:

$$\frac{dA}{dt}\Big|_{cu} = \frac{A^{*} - A^{+}}{\delta t} \tag{6}$$

where the subscript cu denotes the cumulus contribution. The quasi-equilibrium assumption allows as to determine the amount of mass flux M_c by the following:

and closes the parameterization system.

$$\frac{dA}{dt}\Big|_{ls} + M_c \frac{dA}{dt}\Big|_{cu} \approx 0 \tag{7}$$

Finally, the feedback of the cumulus onto the large scale environment is done via the mass flux in the subsidence and the entrainment-detrainment process for moist static energy and for moisture:

$$\rho\frac{\partial h}{\partial t}=E(h-\tilde{h})+D(\tilde{h}-h)+M_c\frac{\partial h}{\partial z} \tag{8}$$

$$\rho\frac{\partial q}{\partial t}=E(q-\tilde{q})+D(\tilde{q}+l-q)+M_c\frac{\partial q}{\partial z} \tag{9}$$

where the terms multiplying the entrainment mass flux (**E**) applies only over the entraining layers and the terms multiplying the detrainment mass flux (**D**) applies only over the detraining layers. The change in temperature can be obtained from Eqs. (8) and (9).

3. Results

We tested the new mass flux scheme in stand alone forecasts and in forecasts initialized by an independent data assimilation system (our parallel system) that is identical to the operational Global Data Assimilation System (GDAS) in every way except the convection scheme. This method removes any spin up/down problem due to the difference in physics. In general, the tropical moisture field tends to be on the dry side when running the mass flux scheme than when running the Kuo scheme. A forecast using the mass flux scheme that is based on an initial condition generated from a GDAS using the Kuo scheme will start out will a large amount of precipitation for 1-2 days. While this may be acceptable in GCM studies, it makes comparison nearly worthless for short and medium range forecasts. During the Spring and Summer of 1993, we had an opportunity to run the mass flux scheme in the parallel for nearly four months, an unusually long time because of a delay in the implementation schedule. Most of the results we show will be from this period.

In addition, we made many 30-day prediction experiments to examine the precipitation pattern over the global tropics. We have become aware for some time now that the MRF running with the Kuo scheme under-predicts the precipitation in the warm tropical ocean when compared with satellite derived precipitation (a product of the Global Precipitation Climatology Project - GPCP) based on Arkin and Meisner (1987). The precipitation rate of GPCP is derived from the satellite measured Outgoing Longwave Radiative flux and probably over-estimates precipitation where high cirrus stays around and under-estimates precipitation where clouds are shallow. Nonetheless, it is the only global measure that has a good coverage of the tropical ocean.

We have also made special data assimilation experiment using the enhanced data collected during the Tropical Cyclone Motion Experiment (TCM90, Elsberry, 1990) to study the response of the tropical storms to the convection scheme change. Four-time daily data assimilation using the operational system (as of March, 1993) and a parallel system have been made for the period 25 August - 19 September 1990. A series of three-day predictions were made using each system for the period 5-16 September 1990. The storm position for each forecast is determined using an objective method and the forecasted track error is determined from an official best track.

a) Precipitation distribution

It has been known to us for some time that precipitation forecasts made with the Kuo scheme have a tendency to be noisy. The degree of noisiness increases with the length of the forecast. Saha and Kanamitsu (1991) demonstrated this problem by examining the forecast precipitation in a two-dimensional wavenumber domain. They showed that the variance in the wavenumber 20-80 range increases with forecast length. A graphical example of this phenomenon is presented in Fig. 1 where the 24-hour accumulated precipitation of a pair of day-5 forecasts are displayed. The forecast using the Kuo scheme (Fig. 1a) shows many concentrated center of high precipitation amounts. The forecast using the new mass flux scheme (Fig. 1b) shows a higher degree of spatial coherency. The forecasts are taken out of the daily MRF forecast and the parallel system. The tendency of the precipitation to cluster in the Kuo forecasts is diagnosed to be due to the feedback mechanism between the convection scheme and the environment. The Kuo scheme uses the low-level moisture convergence to determine the amount of heating and precipitation. When there is low level convergence, the air column heats up and the surface pressure lowers. This leads to more convergence and more precipitation. While this happens in nature to some degree, we believe the use of moisture convergence in the Kuo scheme over-enhanced the interaction. Emanuel (1987) has also criticized the use of large-scale convergence as a criterion for the formation of convection.

In Fig. 2 we present a six-day average of the precipitation variance in the two-dimensional wavenumber domain following Saha and Kanamitsu for the MRF and the parallel system. Day one and day five 12-hour accumulated precipitation forecasts are shown. It can be seen that the variance in the 20-80 wavenumber range increases as a function of the forecast length for the MRF but stay the same for the parallel forecast. Moreover, the variance in this range is much smaller for the parallel system than the operational system which corroborates well with the results shown in Fig. 1. In examining time-longitude Hovmuller diagram of the precipitation field (not shown), the operational system produces many tropical disturbances only some of which can be identified with a satellite picture. The mass flux scheme does not seem to suffer that problem.

b) Short range precipitation forecasts

As the regional modeling effort focuses more and more on meso-scale short-range (12-24 hour) predictions, the global model will be counted to provide forecasts in the 1-3 day range as well. This creates a new challenge to the MRF to provide realistic precipitation forecasts for the North America region. Using the NOAA River Forecast Center's large rain-gauge network for the lower 48 states, NMC has the ability to examine the precipitation performance for this area. The observations are taken at the 12 GMT cycle and are collected by the Office of Hydrology of the National Weather Service. At NMC, a simple precipitation analysis is performed on a delay basis (3-4 days) to produce a verification field. The analysis is performed on the grid point system of each model to be verified and is a simple average of all observed precipitation within each grid box. Both the MRF forecast and the parallel forecast for the 12-36 hour range are archived (both forecasts are run from the 00 GMT cycle) and monthly bias and equitable threat score (Gandin and Murphy, 1992) are obtained.

In Fig. 3, the equitable threat score for the month April, 1993 for the MRF and the parallel (MRX) system is presented and the bias of the precipitation forecast is presented in Fig. 4. The scores are collected for eight precipitation amount categories (.01 .1 .25 .5 .75 1 1.5 2"). It can be seen from Fig. 3 that the mass flux parameterization performed better in all but the very high amount categories. It has been our observation that the MRF system tends to produce more higher amount forecasts while the MRX system tends to produce smoother and less concentrated forecasts. As can be seen in Fig. 4, the bias for the MRF forecasts in the high amount categories are significantly larger than one (the ideal bias) while the MRX forecasts actually becomes less than one. A similar set of scores for the month of May is shown in Figs. 5 and 6. It can be seen that the advantage of the MRX system in the lesser amount categories is maintained while there is a reversal of results in the higher amount categories. Since the number of events in the higher amount categories is much less than those in the lower categories and since the scores are very low for the higher categories, the result signifies that neither system has any skill in these categories. The scores for the months of June and July are similar to the ones shown and will not be shown here.

c) Hurricane track prediction

We ran the GDAS for both systems for 11 days(25 August - 4 September, 1990) to allow the moisture climate of the system to adjust to each convection scheme. For the period 5 September to 16 September 1990, we performed 12 72-hour forecasts (one per day). While there are only a total of 6 tropical cyclones during this period, each were of sufficient duration that five to ten forecasts were obtained for each storm. By also grouping the forecast errors by the storm basin (the Atlantic, the Western Pacific, and the Eastern Pacific), we feel slightly more comfortable with the significance of the results.

The average storm track forecast error for each basin is given in Figs. 7, 8, and 9. In general, the forecasts are better for Western Pacific storms (Fig. 7) and the mass flux scheme performs much better in Western Pacific. The forecasts for Atlantic basin (Fig. 8) is less impressive but the mass flux scheme generally produced a significant reduction in the track error. For the Eastern Pacific basin (Fig. 9), the track forecast errors are also large with the mass flux scheme producing only slight improvement. Our feeling is that the western

Pacific storms tend to be more intense and are easier to predict. The Atlantic and eastern Pacific storms are generally weaker and the tracks are more difficult to predict.

d) Tropical climate sensitivities

In Figs. 10 and 11, the accumulated precipitation from a pair of T62 30-day prediction runs using the Kuo and the mass flux scheme are shown. It can be seen that the prediction using the Kuo scheme (Fig. 10) produces more precipitation over the eastern Pacific Inter-Tropical Convergence Zone (ITCZ) than over the western Pacific while the mass flux scheme (Fig. 11) shifts more precipitation toward western Pacific. Comparing these results with the GPCP climatology for July based on six years of satellite observation (Fig. 12) would suggest that the new scheme provides a better tropical climatology than the Kuo scheme. Quantitatively, both schemes under-estimates the amount of precipitation compared with the GPCP observations. At the same time, both schemes produce too much precipitation over the maritime continents. While the mass flux scheme produces less convective precipitation over the islands (and the high tropical mountains), the large scale precipitation package in the model picks up the rest to produce about the same amount of total precipitation in the end. This is a problem that requires examination of other packages of the model.

One method to summarize the tropical precipitation distribution is to group the precipitation with respect to the underlying SST field. The 30-day prediction experiments are presented in Fig. 13. The Kuo scheme produces more precipitation in the 22-27 ^{0}C range than the mass flux scheme and less in the warmer water region while both are considerably less than the GPCP observations. A single 5-day prediction pair taken from the parallel test using both T126 and T62 resolution is shown in Fig. 14 and the difference between the two is fairly small suggesting that the mass flux scheme is not sensitive to model resolution. Over land (not shown), the difference is larger and reflects the importance of surface inhomogeneity.

An attempt has been made to further improve the precipitation-SST relationship in the mass flux scheme by re-examining the climatological cloud work function used in the scheme.

The original climatology was derived by Lord using Marshall Island data and the Arakawa-Schubert scheme. In data assimilation experiment, we noticed that the cloud work function in the analysis never approached the specified climatology. This is especially true for the shallower clouds. Lord (personal communication) suggested that the climatology for the shallower clouds may be less reliable because the sample size was smaller. We have, therefore, re-calculated the climatology using the new mass flux scheme and one month (August 1985) of four-times daily global analysis data. The results are shown in Fig. 15 and the values are generally larger than the results of Lord but especially so for the shallower clouds. We have also examined the globally averaged cloud work function for other seasons and resolutions and the results are very similar to that shown in Fig. 15. Running with the new cloud work function climatology does improve the tropical precipitation-SST relationship (Fig. 16) but only marginally. Globally averaged convective heating profile from the analysis for the second half of the month (Fig. 17) shows that the convective heating below about 600 hPa is indeed smaller for the new climatology. The large-scale super-saturation heating (Fig. 18) however compensated for that so that the total heating due to condensation (Fig. 19) is about the same. The reason for this is not clear immediately and we plan to examine it further in the near future.

4. Summary and Conclusions

A much simplified mass flux scheme that is based on the work of Arakawa and Schubert (1974), Lord (1978), and Grell (1993) has been tested in the NMC MRF model. The new scheme adds 10-15 % of cpu time to the model run time and must be justified with better performance before implementation can be considered. In GDAS (not shown for brevity), the scheme has shown much less spin-up in the precipitation forecast and has less cold bias in the tropics. In short range precipitation forecast for the lower 48 states of U.S., the new scheme provides a very even bias in most of the categories and scores consistently better in almost all categories. While the score is still not as good as the regional Eta model, it is very competitive with both the NGM and the Eta model. In prediction of the tropical storm track, the new scheme also performed slightly better that the Kuo scheme. With a limited sample, we are unable to diagnose the reason for the improvement. Further work is required in this area.

The tropical precipitation pattern generated with extended period runs with the MRF model showed that the new scheme simulates a more realistic precipitation - SST correlation. While the precipitation over warm SST region is still lacking compared with observation, it represents a first step toward better prediction of the tropical precipitation. The tropical precipitation is also shown to be not so sensitive to model resolution, allowing us to do further studies using lower resolution models. Another feature that the new scheme has improved is the tropical cold bias. The MRF has long had a tropical cold bias with a zonal mean 500 hPa height field in the tropics 20 meters below climatology in the day-5 forecast. The new scheme has reduced that bias to 5-10 meters.

While there were many aspects where the new mass flux scheme has performed better than the older scheme, we have certainly not made everything better. The 500 hPa day-5 anomaly correlation coefficient, a score that has long been the gauge of improvement of the MRF forecasts, showed no improvement. In fact, the score was usually 1-2 percentage point worse. We felt that many of the model parameters have been adjusted based on the Kuo scheme since it has such a long presence in the model. By making a drastic change in the convection scheme, we may now have to reexamine these parameters in the other parameterization packages. Such work will probably go on during the next year or so.

The MRF still produces precipitation centers over the tropical mountains. While the convective precipitation has been reduced drastically, the large-scale supersaturation precipitation has compensated for it. This is a problem of clouds, solar radiation and sensible heat flux at the surface and may require an improved surface physics and cloud prediction to finally solve the problem. We have also noted that the model has, on occasion, produced very concentrated precipitation centers over the mid-west region of the United State. This phenomenon has been observed in spring and in autumn. The few times that we have observed this occurrence, there were usually severe weather outbursts in reality. Diagnosis of the model behavior reveals that the model simulated convection is weak while the large scale super-saturation heating takes place over a very deep layer. The same forecast made with a low resolution model (T62) showed more convective precipitation but no super-saturation precipitation. As the model resolution gets near the so-called meso-scale convective complex scale, the question of the closure must be re-examined.

As we reduce the complexity of the cloud model that is used in the static control from an ensemble of clouds to a single cloud with very simple entrainment and detrainment properties, it becomes clear that the closure selection is the central problem of this simple parameterization scheme. The cloud scale stabilization effect depends on the mass flux which we hope to deduce from the large scale destabilization effect. Lord (1978) provided the first practical closure as an adjustment of the cloud work function toward a climatology that he derived from observation. Tiedtke (1989), Gregory and Rowntree (1990), and Grell (1993) all have different closure scheme that are based on other physical arguements. Obviously, the problem of the closure is far from being resolved. The central question we must answer is the time scale on which the convection will remove the conditional instability. While the tropical atmosphere remains conditionally unstable even after the passage of disturbances, mid-latitude summer time thunderstorms strongly stablizes the atmosphere. Ideally, the large scale destabilization should be specified as the rate at which the given instability of an air column will be neutralized and should be different based on the large scale forcing of the environment while the restoration of the instability is done by other physical processes such as radiation, surface interaction, and boundary layer turbulent mixing. When we use a closure that adjusts toward climatology, we are not allowing the other restoring mechanism to perform their functions.

While the non-entraining cloud assumption probably works for deep convective systems, it definitely is not the case for shallower clouds and we need to modify the cloud properties for these clouds in the future. The model is written such that the entraining and detraining properties of the clouds can be changed easily to allow experimentation on them.

Based on the results presented in this paper and the results of various diagnostic work performed by the Development Division staff, the new mass flux scheme was implemented into the operational MRF model on 11 August 1993.

Acknowledgments. We gratefully acknowledge the support and guidance of E. Kalnay throughout the last two years while the development work was done. We are thankful for the insistence of both M. Kanamitsu and S. J. Lord that we compromise as little as possible and for their encouragement. Discussions with S. K. Esbensen, and P. Caplan have resulted in improvements in the scheme. R. Kistler, E. Rogers, Y. Zhu, and H. Juang all provided assistance in the many experiments we performed for this study and we are deeply grateful for their help.

REFERENCES

Arakawa, A., and W. H. Schubert, 1974: Interaction of a cumulus ensemble with the large-scale environment, Part I. *J. Atmos. Sci.*, **31**, 674 - 701.

Arkin, P. A., and B. N. Meisner, 1987: The relationship between large-scale convective rainfall and cold cloud over the western hemisphere during 1982-84. *Mon. Wea. Rev.*, **115**, 51-74.

Betts, A. K., and M. J. Miller, 1986: A new convective adjustment scheme. Part II: Single column tests using GATE wave, BOMEX, ATEX and arctic airmass data sets. *Quart. J. Roy. Meteor. Soc.*, **112**, 692-709.

Charney, J. G., and A. Eliassen, 1964: On the growth of the hurricane depression. *J. Atmos. Sci.*, **21**, 68-75.

Cheng, M. -D., and A. Arakawa, 1990: Inclusion of convective downdrafts in the Arakawa-Schubert cumulus parameterization. Tech. Rept., Dept. of Atmospheric Science, University of California at Los Angeles, 69pp.

Elsberry, R. L., 1990: International experiments to study tropical cyclones in the western North Pacific. *Bull. Amer. Metero. Soc.*, **71**, 1305-1316.

Emanuel, K. A., 1987: Large-scale and mesoscale circulations in convectively adjusted atmospheres. Workshop on Diabatic Forcing, ECMWF, Reading, England, 323-348.

Fristch, J. M., and C. F. Chappel, 1980: Numerical prediction of convectively driven mesoscale pressure systems. Part I: Convective parameterization. *J. Atmos. Sci.*, **37**, 1722-1733.

Gandin, L. S., and A. H. Murphy, 1992: Equitable skill scores for categorical forecasts. *Mon. Wea. Rev.*, **120**, 361-370.

Gregory, D. and P. R. Rowntree, 1990: A mass flux convection scheme with representation of cloud ensemble characteristics and stability-dependent closure. *Mon. Wea. Rev.*, **118**, 1483-1506.

Grell, G. A., 1993: Prognostic evaluation of assumptions used by cumulus parameterizations. *Mon. Wea. Rev.*, **121**, 764-787.

Kanamitsu, M., J. C. Alpert, K. A. Campana, P. M. Caplan, D. G. Deaven, M. Idedell, B. Katz, H. -L. Pan, J. Sela, and G. H. White: 1991: Recent changes implemented into the global forecast system at NMC. *Wea. Forecasting*, **6**, 425-435.

Kuo, H. -L., 1965: On formation and intensification of tropical cyclones through latent heat release by cumulus convection. *J. Atmos. Sci.*, **22**, 40-63.

Kuo, H. -L., 1974: Further studies of the parameterization of the influence of cumulus convection on large-scale flow. *J. Atmos. Sci.*, **31**, 1232-1240.

Lord, S. J., 1978: Development and observational verification of cumulus cloud parameterization. Ph. D. dissertation, University of California, Los Angeles, 359pp.

Mesinger, F., Z. I. Janjic, S. Nichovic, D. Garrilor, and D. G. Deaven, 1988: The step-mountain coordinate: Model description and performance for cases of Alpine cyclogenesis and for a case of an Appalacian redevelopment. *Mon. Wea. Rev.*, **116**, 1493-1518.

Nitta, T., 1975: Observational determination of cloud mass flux distribution. *J. Atmos. Sci.*, **32**, 73-91.

Phillips, N. A., 1979: The Nested grid model. NOAA Tech. REPT. NWS 22, 80pp.

Saha, S., and M. Kanamitsu, 1991: A study of the spin-up characteristics of the NMC operational and experimental analysis and forecast systems. *Postprints*: Ninth Conference on Numerical Weather Prediction, Denver, Amer. Meteor. Soc., 392-295.

Sela, J. G., 1980: Spectral modeling at the National Meteorological Center. *Mon. Wea. Rev.*, **108**, 1279-1292.

Tiedtke, M., 1989: A comprehensive mass flux scheme for cumulus parameterization in large-scale models. *Mon. Wea. Rev.*, **117**, 1779-1800.

Yanai, M., S. Esbensen, and J. -H. Chu, 1973: Determination of bulk properties of tropical cloud clusters from large-scale heat and moisture budgets. *J. Atmos. Sci.*, **30**, 611-627.

FIGURES

Fig. 1. Model predicted precipitation (inches) over a 24-hour period for a day-5 forecast from 00 GMT 22 July, 1993 using a) the Kuo scheme, and b) the mass flux scheme. The contour intervals are: .03, .25, .5, 1.,2.,4. inches and shading starts at .25 inches.

Fig. 2. Variance (mm^2) of the 12-hour accumulated precipitation in the global wavenumber domain averaged over 6 cases (15 - 20 July, 1993) for A: 24-hour forecast with the Kuo scheme, B: 120-hour forecast with the Kuo scheme, C: 24-hour forecast with the mass flux scheme, and D: 120-hour forecast with the mass flux scheme.

Fig. 3. Equitable threat score for 12 - 36 hour precipitation forecast over the contiguous U. S. for the month of April, 1993 for the Kuo scheme (MRF) and the mass flux scheme (MRX) for eight categories (.01, .1, .25, .5, .75, 1, 1.5, 2 inches).

Fig. 4. same as Fig. 3 except for precipitation bias.

Fig. 5. same as Fig. 3 except for the month of May, 1993.

Fig. 6. same as Fig. 3 except for precipitation bias for the month of May, 1993.

Fig. 7. Tropical storm track forecast error (km) for the period 5 - 16 September, 1990 for the Western Pacific basin for forecast period up to 72 hours.

Fig. 8. same as Fig. 7 except for the Atlantic basin.

Fig. 9. same as Fig. 7 except for the Eastern Pacific basin.

Fig. 10. Accumulated convective precipitation (mm) for a 30-day forecast experiment from 00 GMT 4 July, 1985 using the Kuo scheme. Contour interval is 100 mm and shading starts at 200 mm.

Fig. 11. same as Fig. 10 except for the mass flux scheme.

Fig. 12. GPI precipitation (mm) estimated from satellite for July averaged over 6 years (1986 - 1991). Contour interval is 100 mm and shading starts at 300 mm.

Fig. 13. Monthly mean precipitation (mm) over the tropical ocean (20 °S - 20 °N) categorized over the sea surface temperature for the climatological GPI field (GPCP), the forecast experiment using the mass flux scheme (MRX), and the forecast experiment using the Kuo scheme (MRF). The forecasts are for 30-day period starting at 00 GMT 4 July, 1985.

Fig. 14. Precipitation (mm) over the tropical ocean categorized over the SST for the climatological GPI field (GPCP), the five-day mean T126 resolution model forecast (T126), and the T62 resolution model forecast (T62). The model runs uses the mass flux scheme and are a pair of 5-day forecasts from 00 GMT 14 July, 1993.

Fig. 15. Globally averaged cloud work function ($J\ kg^{-1}$) derived using the mass flux scheme from the 4-times daily analysis fields for the month August, 1985 including updraft only (Updraft), including updraft and downdraft (Total), and the climatology of Lord (Lord-78). The cloud work functions are normalized by the depth of the cloud (hPa).

Fig. 16. same as 13 except for the climatology of Lord (Lord-78) and the climatology derived from the global analysis for the month August, 1985 (New Acrit).

Fig. 17. Globally averaged convective heating function (10^{5} K) from the 4-times daily 6-hour forecasts for the period 16 - 31 August, 1985 for the Lord climatology (closed circles) and the newly derived climatology (open circle). The vertical coordinate is the model sigma

levels.

Fig. 18. same as Fig. 17 except for the large-scale super-saturation heating profiles

Fig. 19. same as Fig. 17 except for the combined convective and large-scale heating.

RAIN FROM 93/7/22/0Z VT 93/7/27/0Z TUE DAY 5 MRF T126(.03,.25,.5,1,2,4")

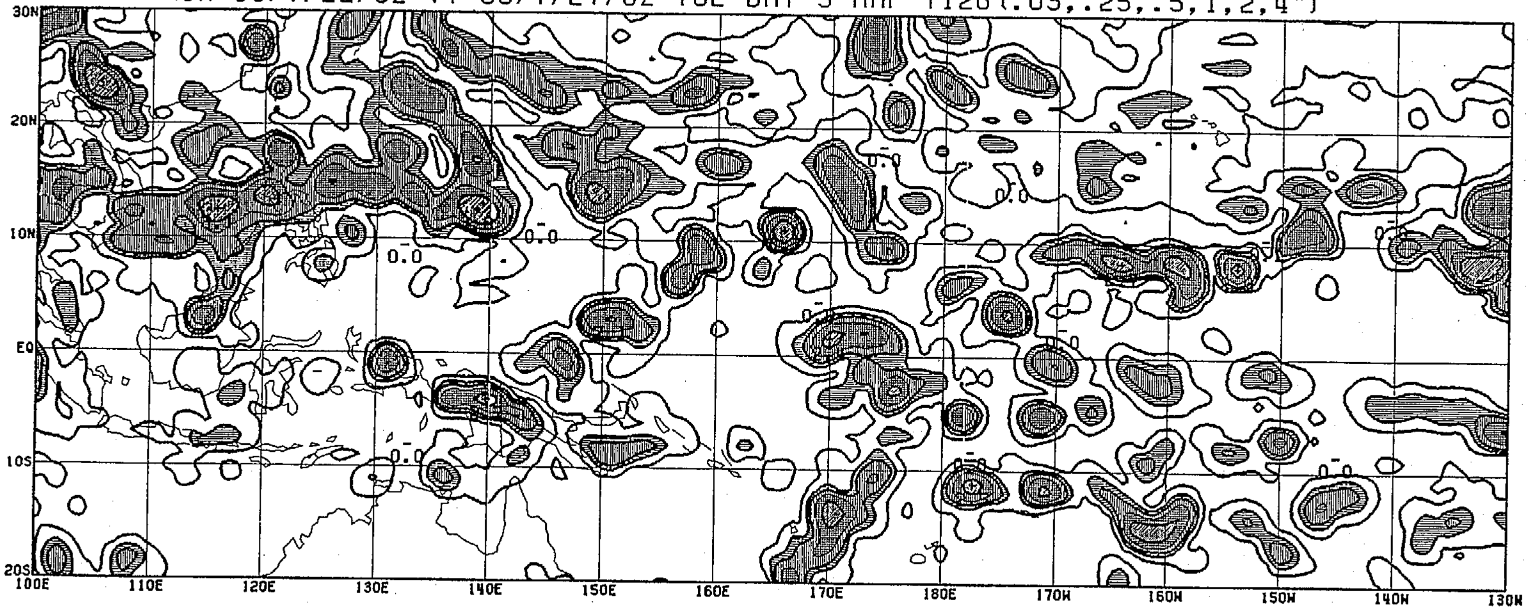

1 a

RAIN FROM 93/7/22/0Z VT 93/7/27/0Z TUE DAY 5 PRX GRELL(.03,.25,.5,1,2,4")

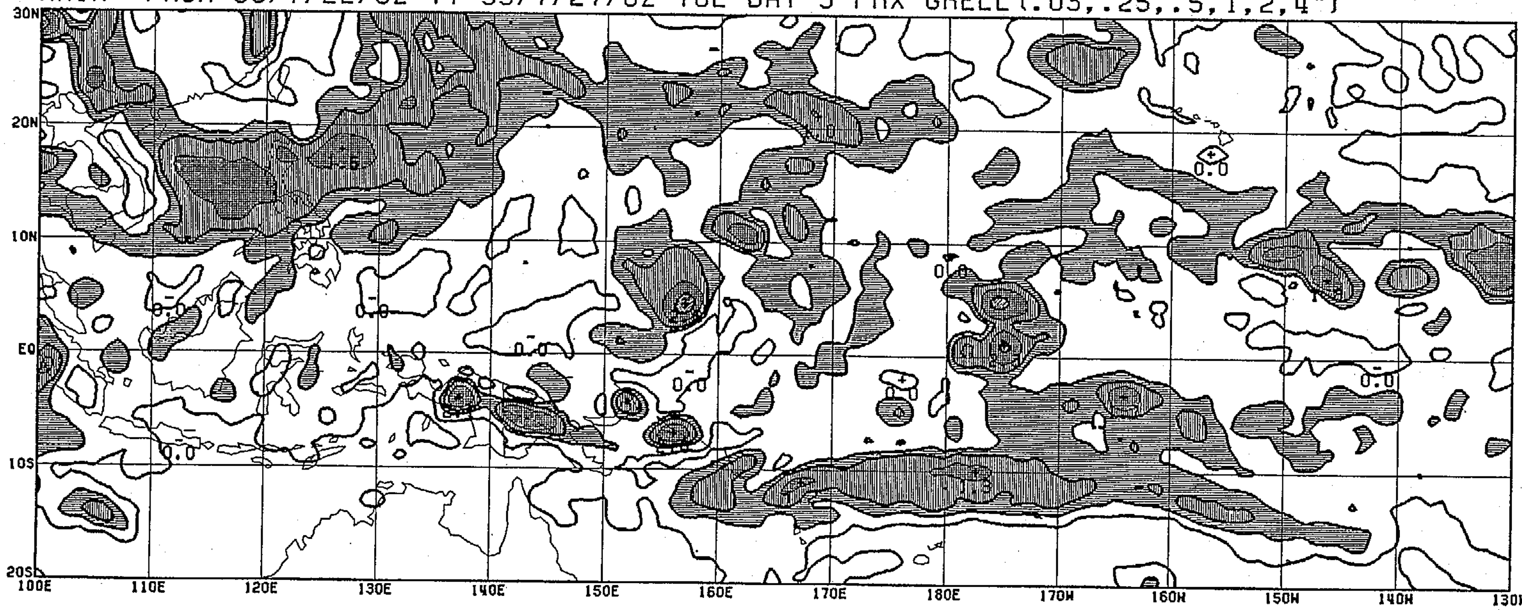

1 b

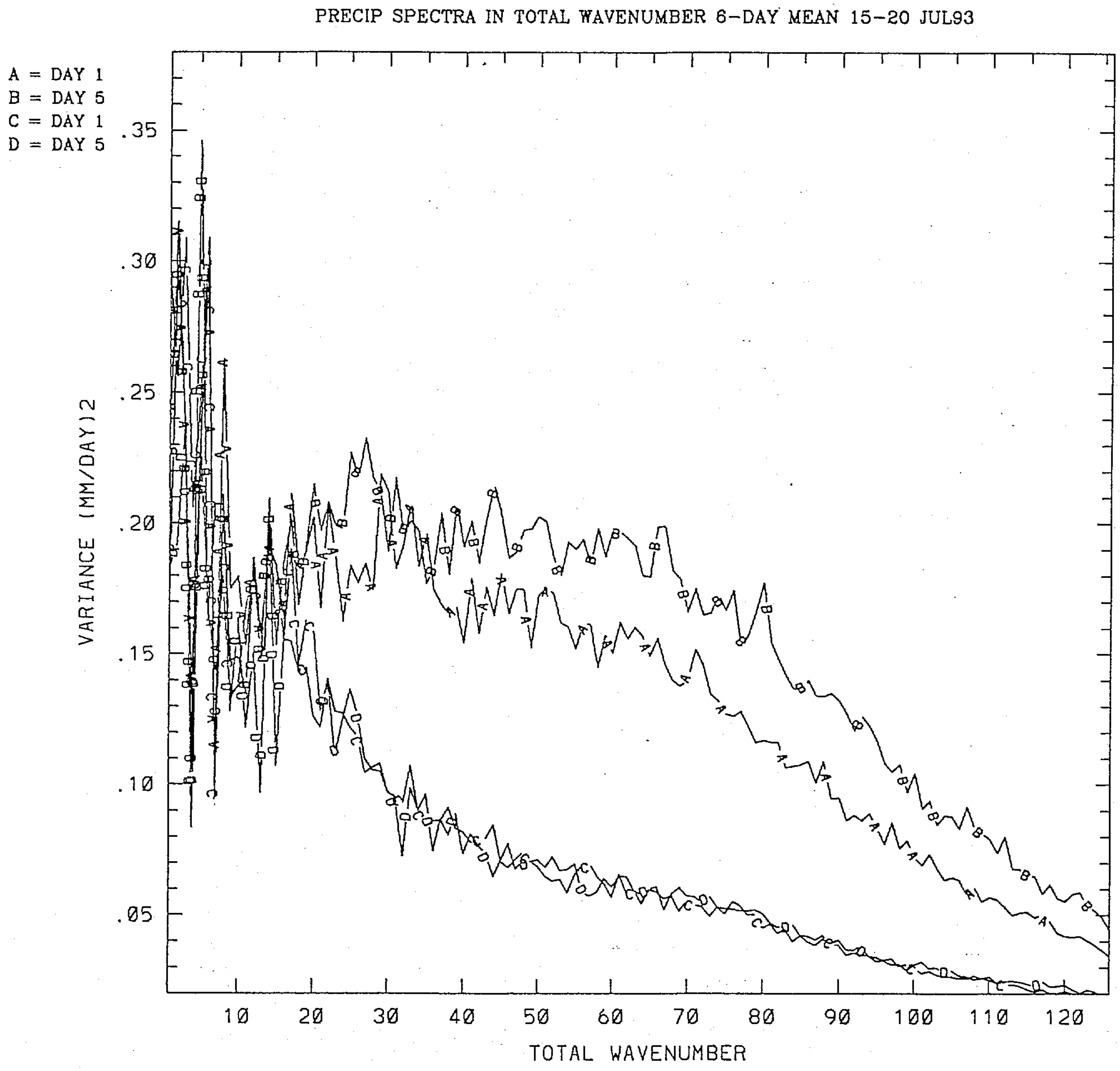
PRECIP SPECTRA IN TOTAL WAVENUMBER 6-DAY MEAN 15-20 JUL93
A = DAY 1
B = DAY 5
C = DAY 1
D = DAY 5
VARIANCE (MM/DAY)2
.05
.10
.15
.20
.25
.30
.35
10
20
30
40
50
60
70
80
90
100
110
120
TOTAL WAVENUMBER

Fig. 2

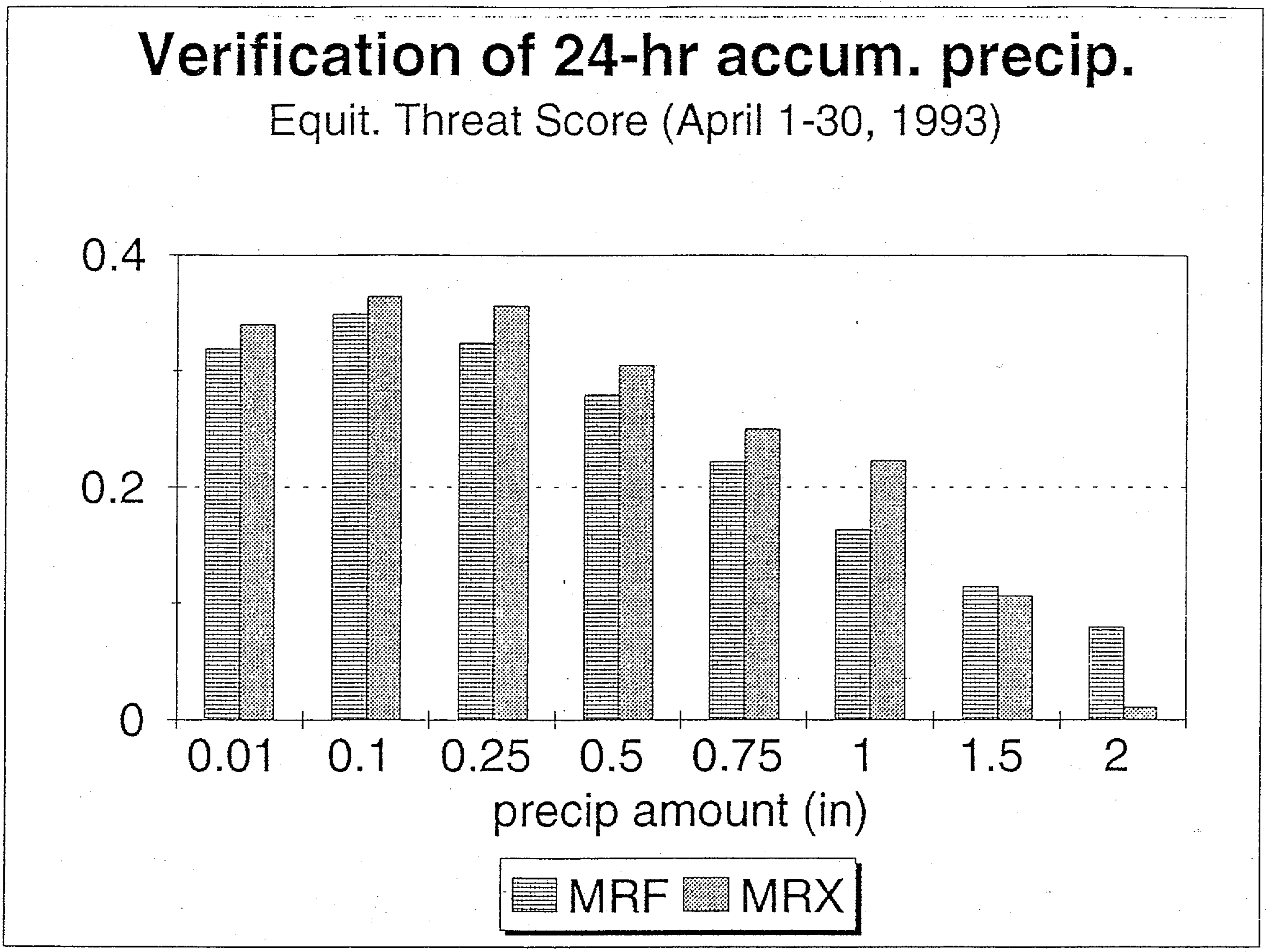

Verification of 24-hr accum. precip.
Equit. Threat Score (April 1-30, 1993)
0.4
0.2
0
0.01
0.1
0.25
0.5
0.75
1
1.5
2
precip amount (in)
MRF
MRX

Fig. 3

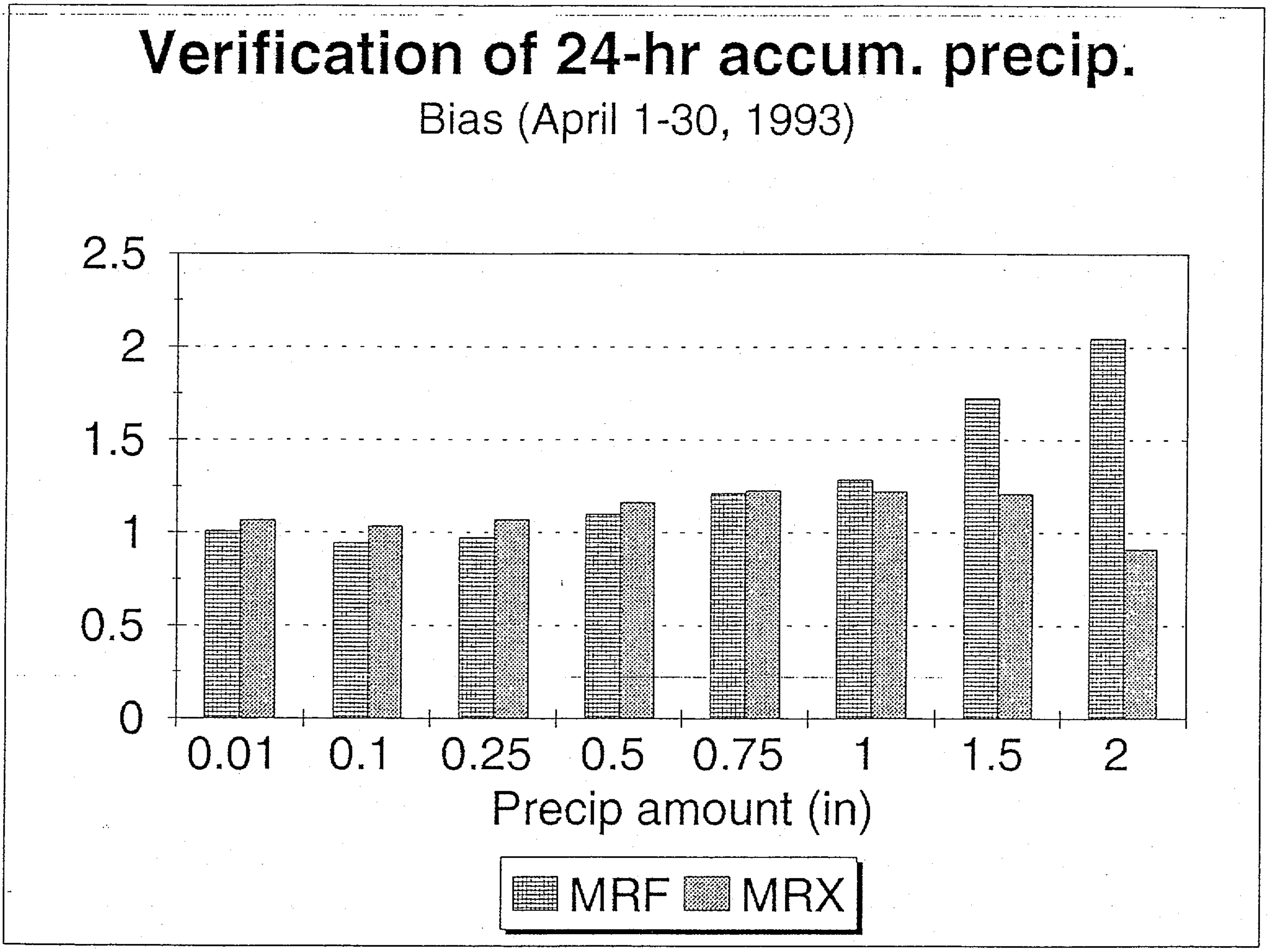
Verification of 24-hr accum. precip.
Bias (April 1-30, 1993)
2.5
2
1.5
1
0.5
0
0.01
0.1
0.25
0.5
0.75
1
1.5
2
Precip amount (in)
MRF
MRX

Fig 4

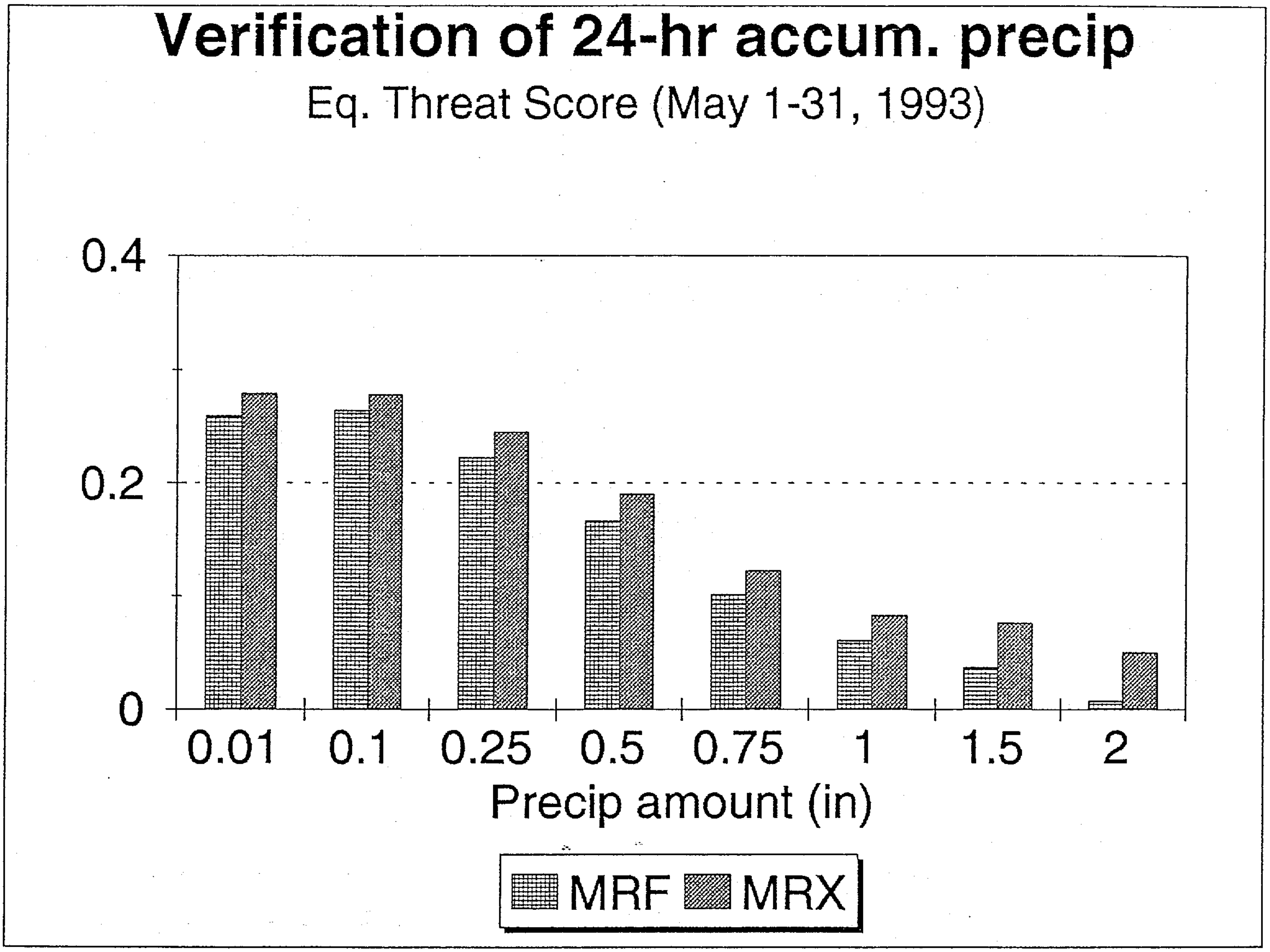
Verification of 24-hr accum. precip
Eq. Threat Score (May 1-31, 1993)
0.4
0.2
0
0.01
0.1
0.25
0.5
0.75
1
1.5
2
Precip amount (in)
MRF
MRX

Fig. 5

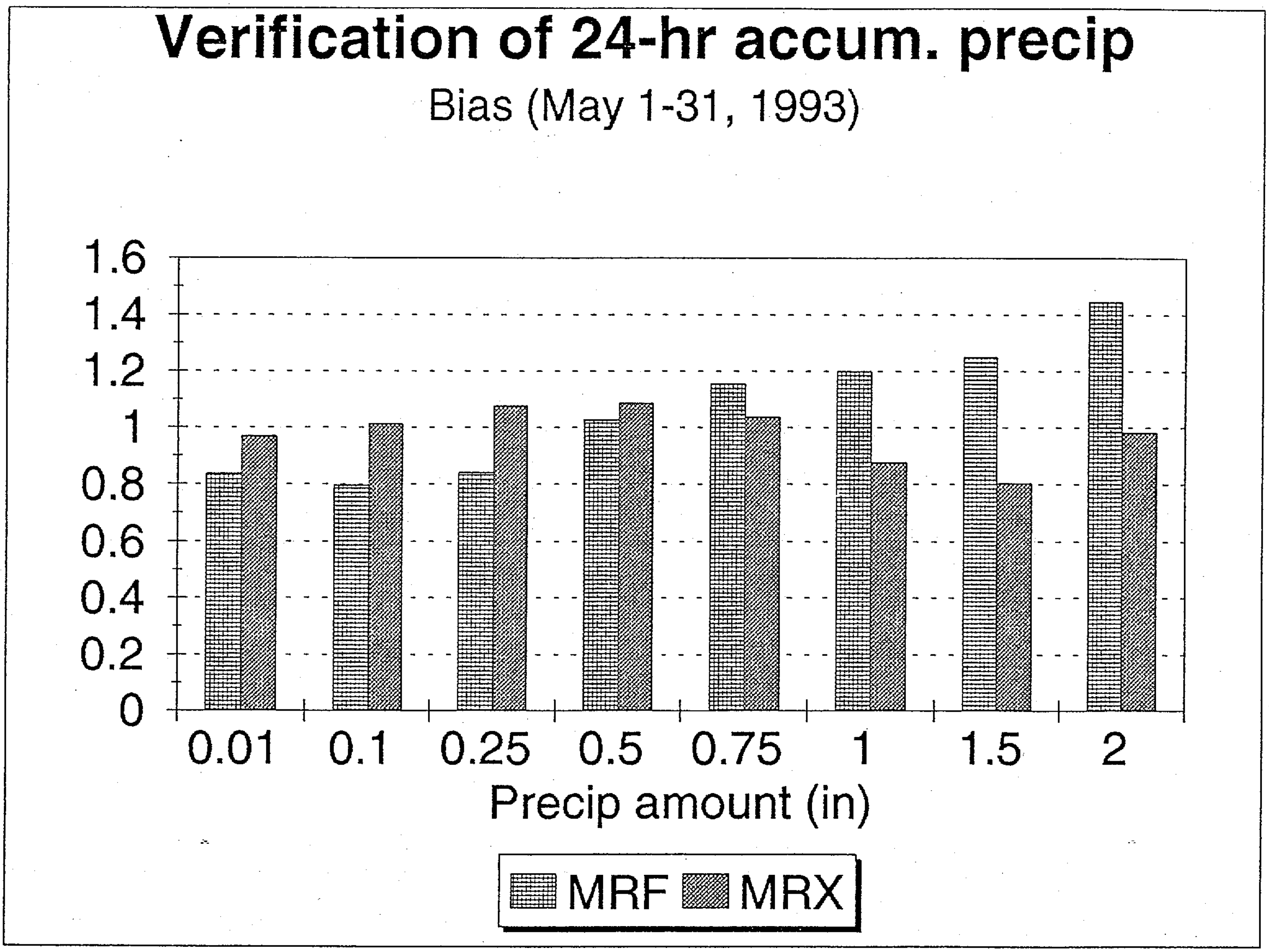
Verification of 24-hr accum. precip
Bias (May 1-31, 1993)
1.6
1.4
1.2
1
0.8
0.6
0.4
0.2
0
0.01
0.1
0.25
0.5
0.75
1
1.5
2
Precip amount (in)
MRF
MRX

Fig. 6

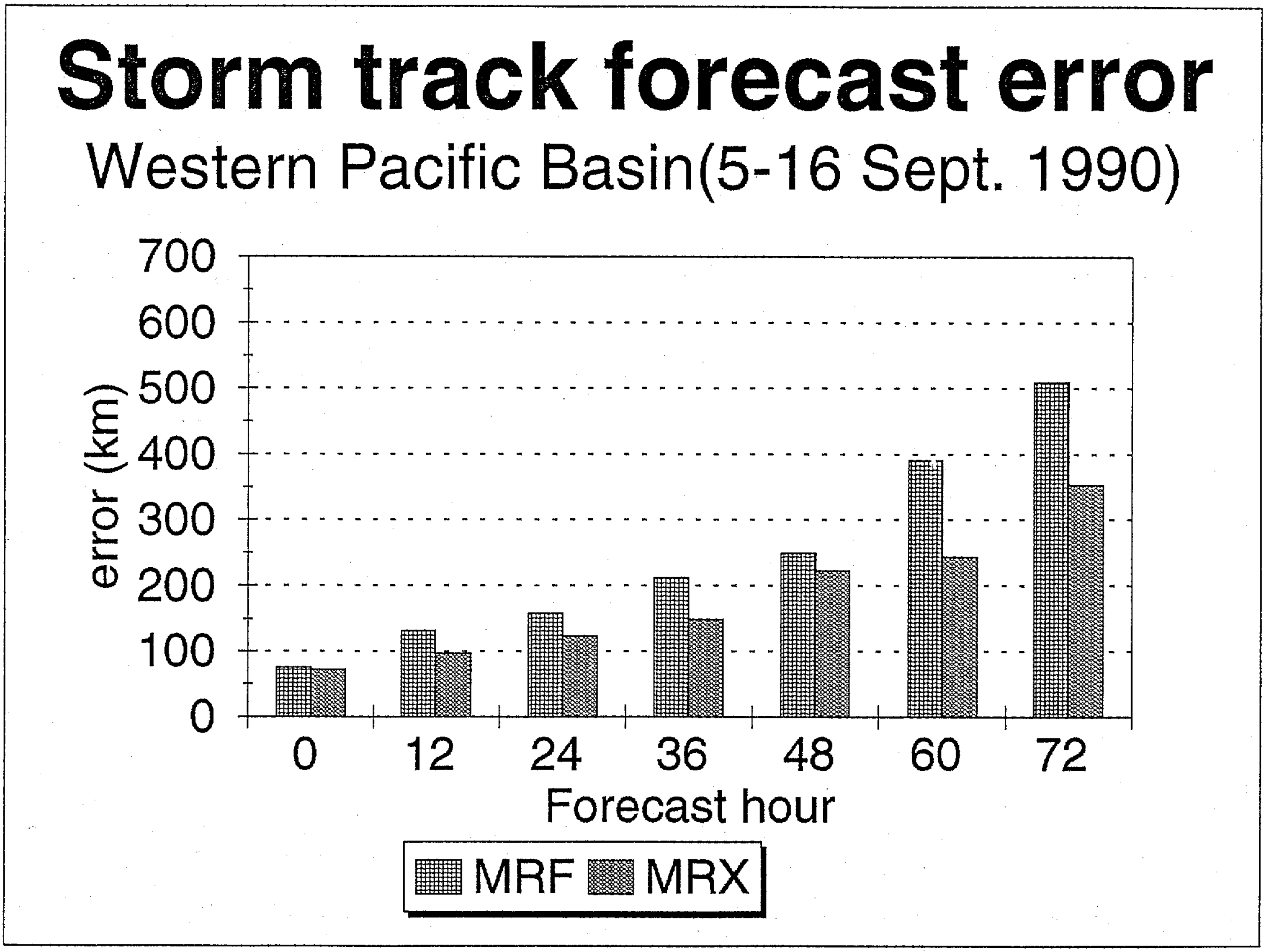
Storm track forecast error
Western Pacific Basin(5-16 Sept. 1990)
700
600
500
400
300
200
100
0
error (km)
0
12
24
36
48
60
72
Forecast hour
MRF
MRX

Fig 7

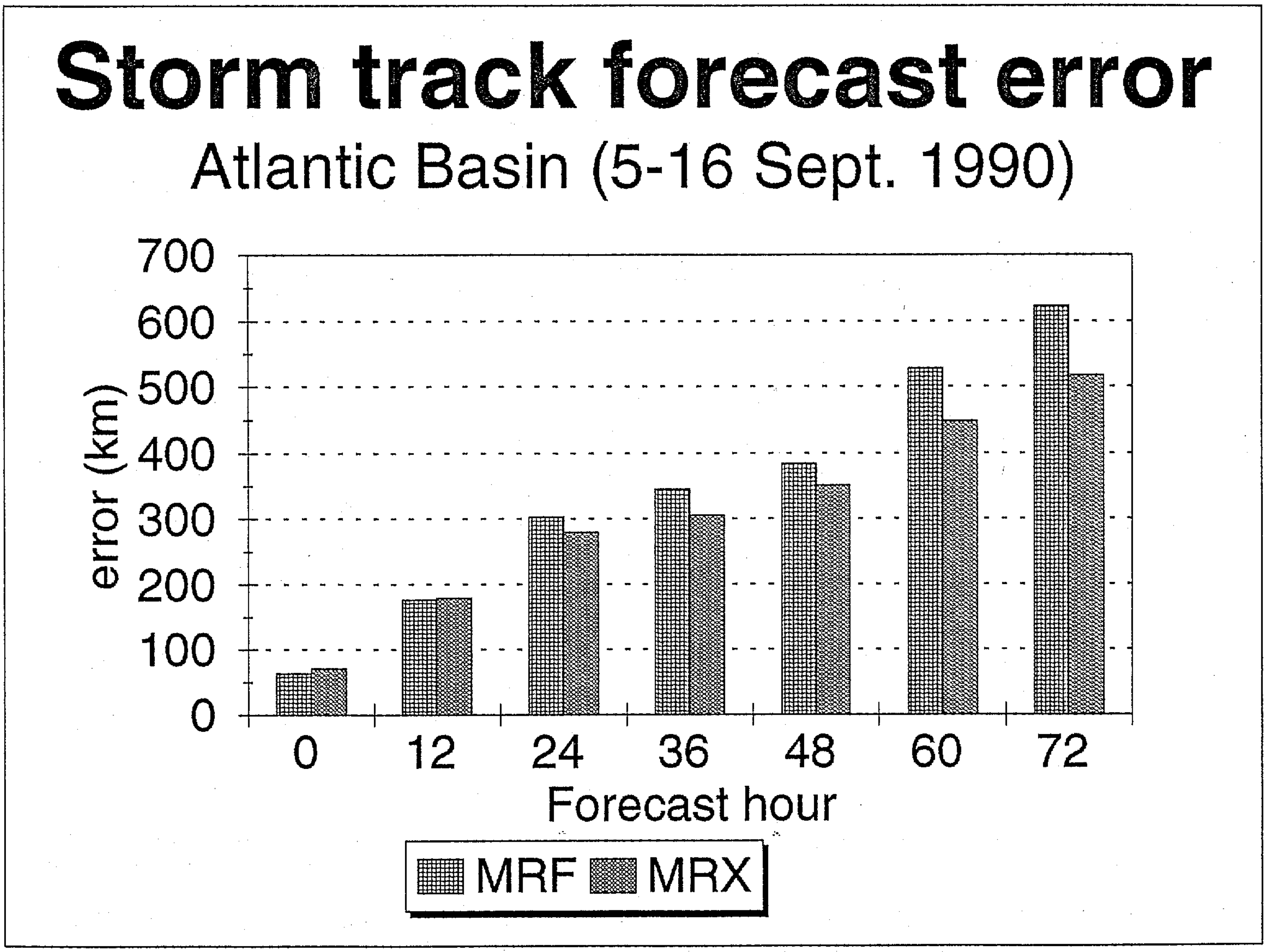
Storm track forecast error
Atlantic Basin (5-16 Sept. 1990)
700
600
500
400
300
200
100
0
error (km)
0
12
24
36
48
60
72
Forecast hour
MRF
MRX

Fig. 8

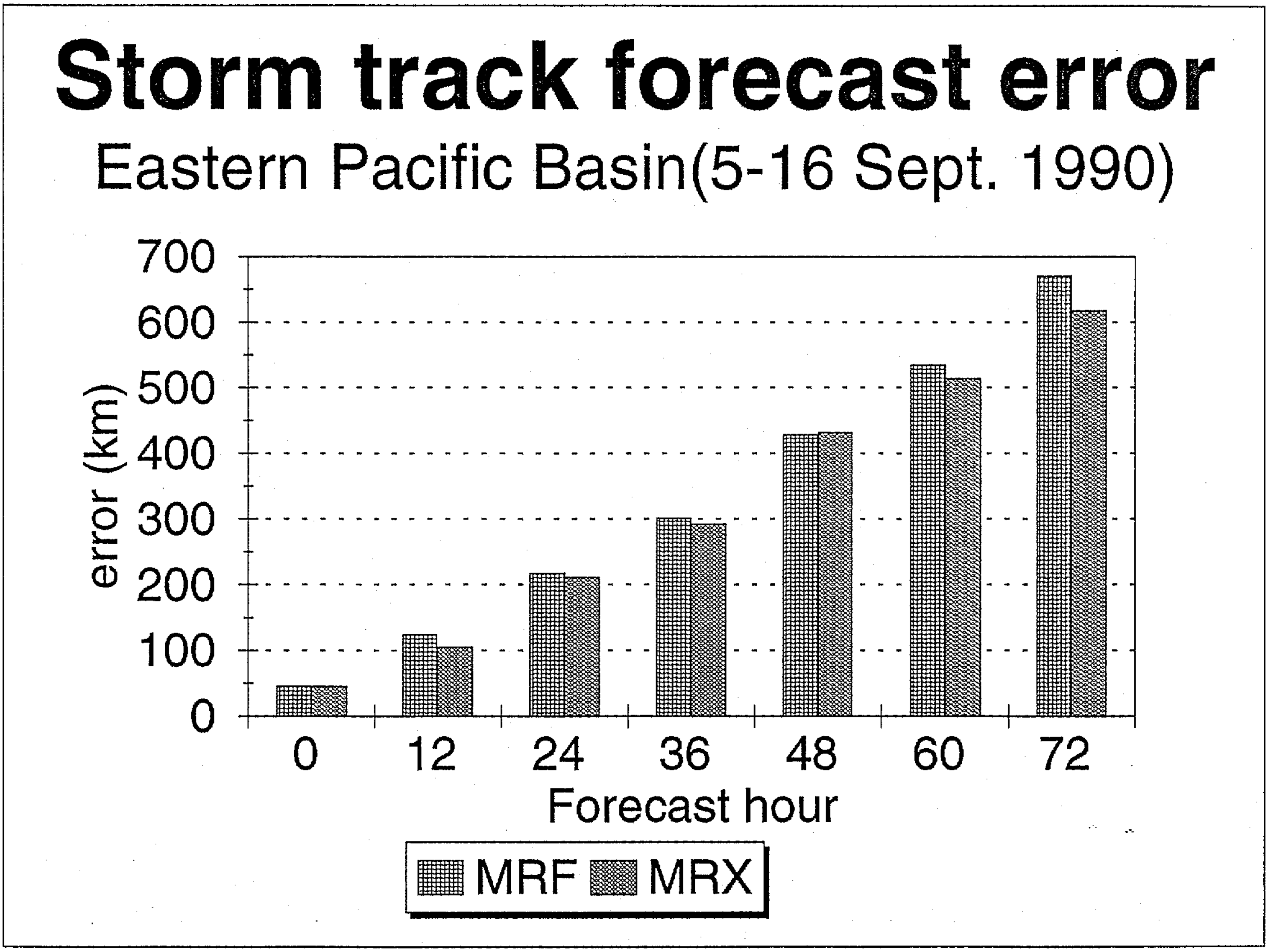
Storm track forecast error
Eastern Pacific Basin(5-16 Sept. 1990)
700
600
500
400
300
200
100
0
error (km)
0
12
24
36
48
60
72
Forecast hour
MRF
MRX

Fig. 9

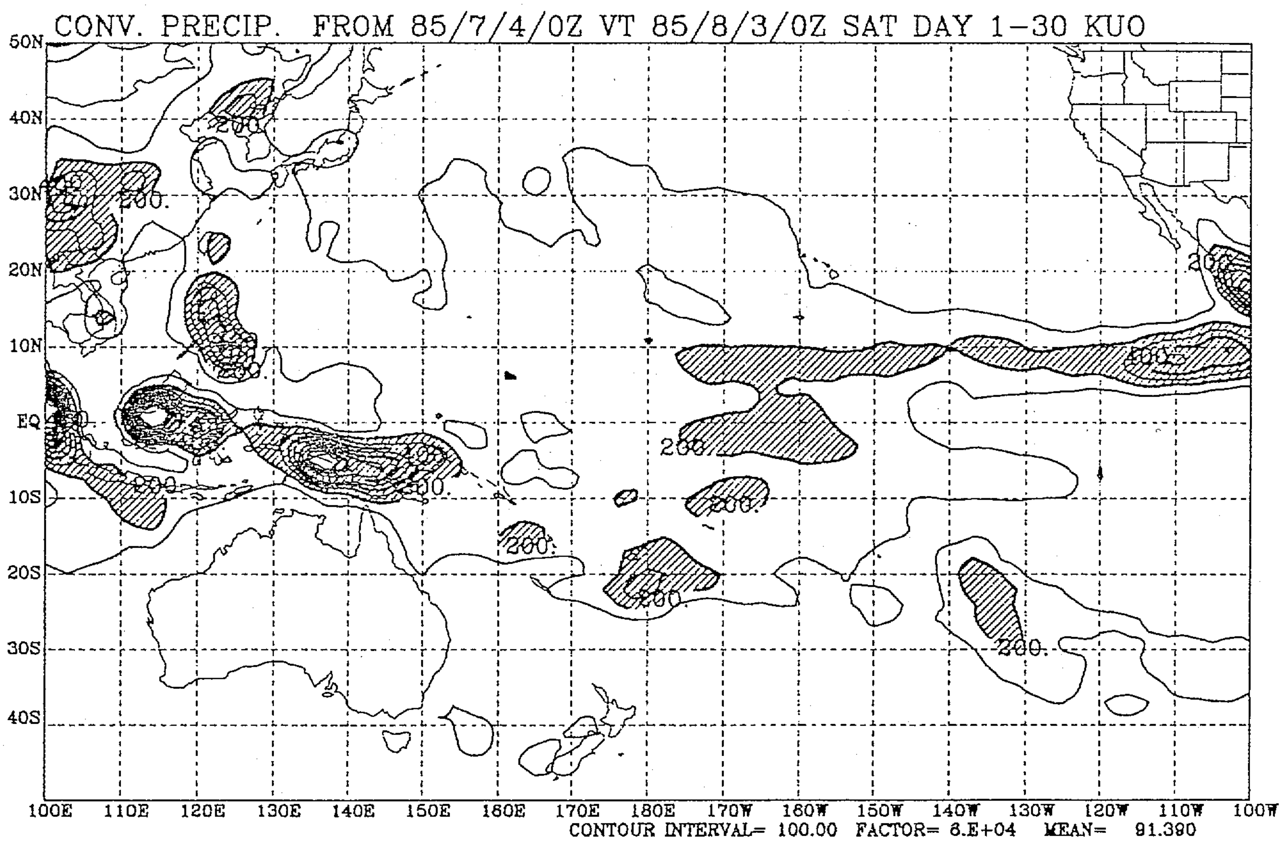
CONV. PRECIP. FROM 85/7/4/0Z VT 85/8/3/0Z SAT DAY 1-30 KUO
50N
40N
30N
20N
10N
EQ
10S
20S
30S
40S
100E 110E 120E 130E 140E 150E 160E 170E 180E 170W 160W 150W 140W 130W 120W 110W 100W
CONTOUR INTERVAL= 100.00 FACTOR= 8.E+04 MEAN= 91.390

Fig. 10

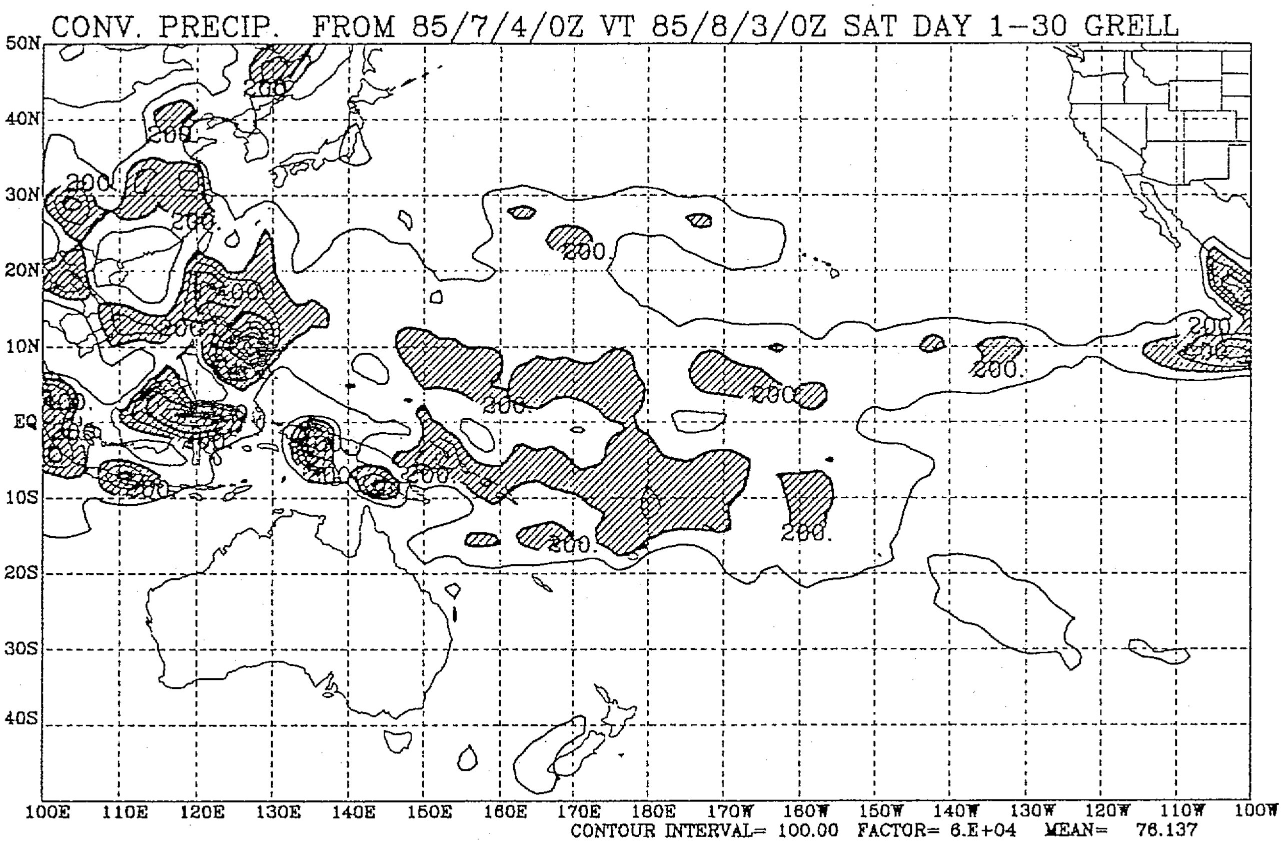
CONV. PRECIP. FROM 85/7/4/0Z VT 85/8/3/0Z SAT DAY 1-30 GRELL
50N
40N
30N
20N
10N
EQ
10S
20S
30S
40S
100E 110E 120E 130E 140E 150E 160E 170E 180E 170W 160W 150W 140W 130W 120W 110W 100W
CONTOUR INTERVAL= 100.00 FACTOR= 6.E+04 MEAN= 76.137

Fig. 11

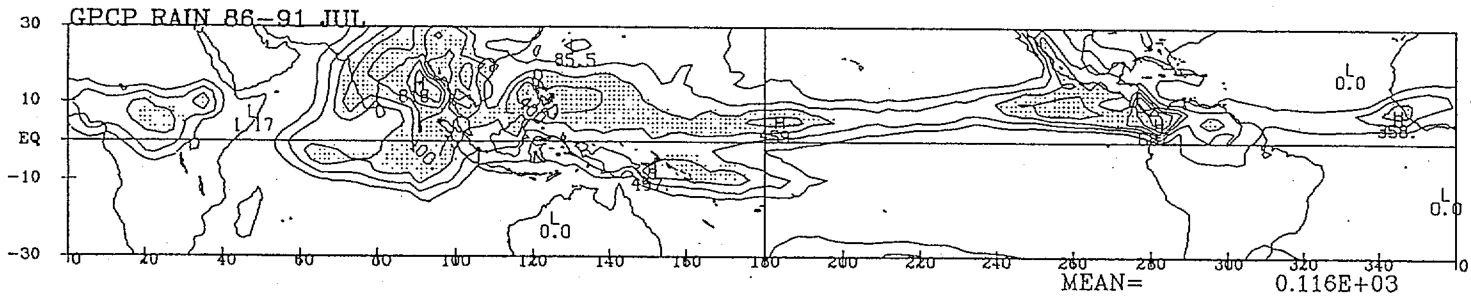
GPCP RAIN 86-91 JUL
30
10
EQ
-10
-30
0
20
40
60
80
100
120
140
160
180
200
220
240
260
280
300
320
340
0
MEAN=
0.116E+03

Fig. 12

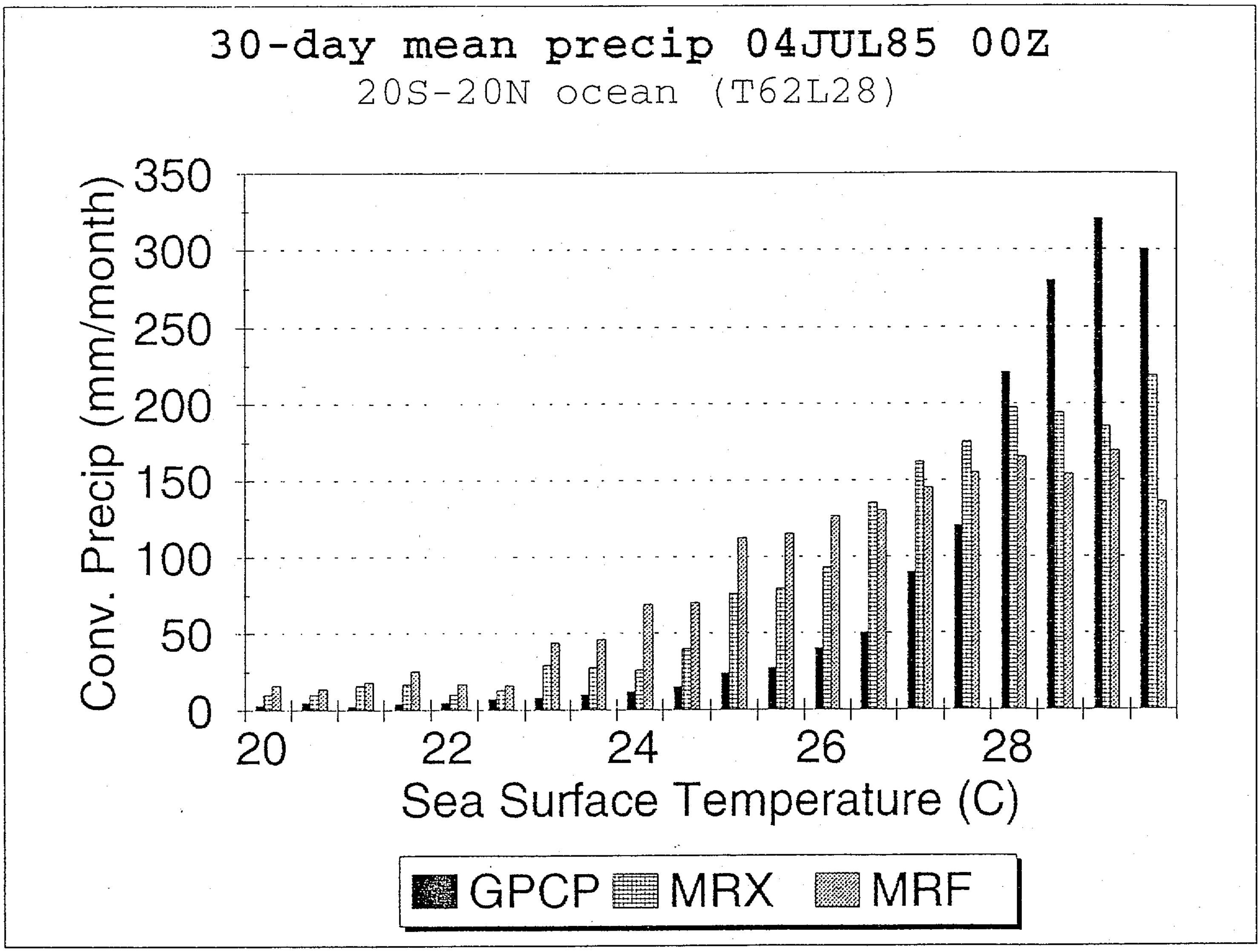
30-day mean precip 04JUL85 00Z
20S-20N ocean (T62L28)
Conv. Precip (mm/month)
350
300
250
200
150
100
50
0
20
22
24
26
28
Sea Surface Temperature (C)
GPCP
MRX
MRF

Fig. 13

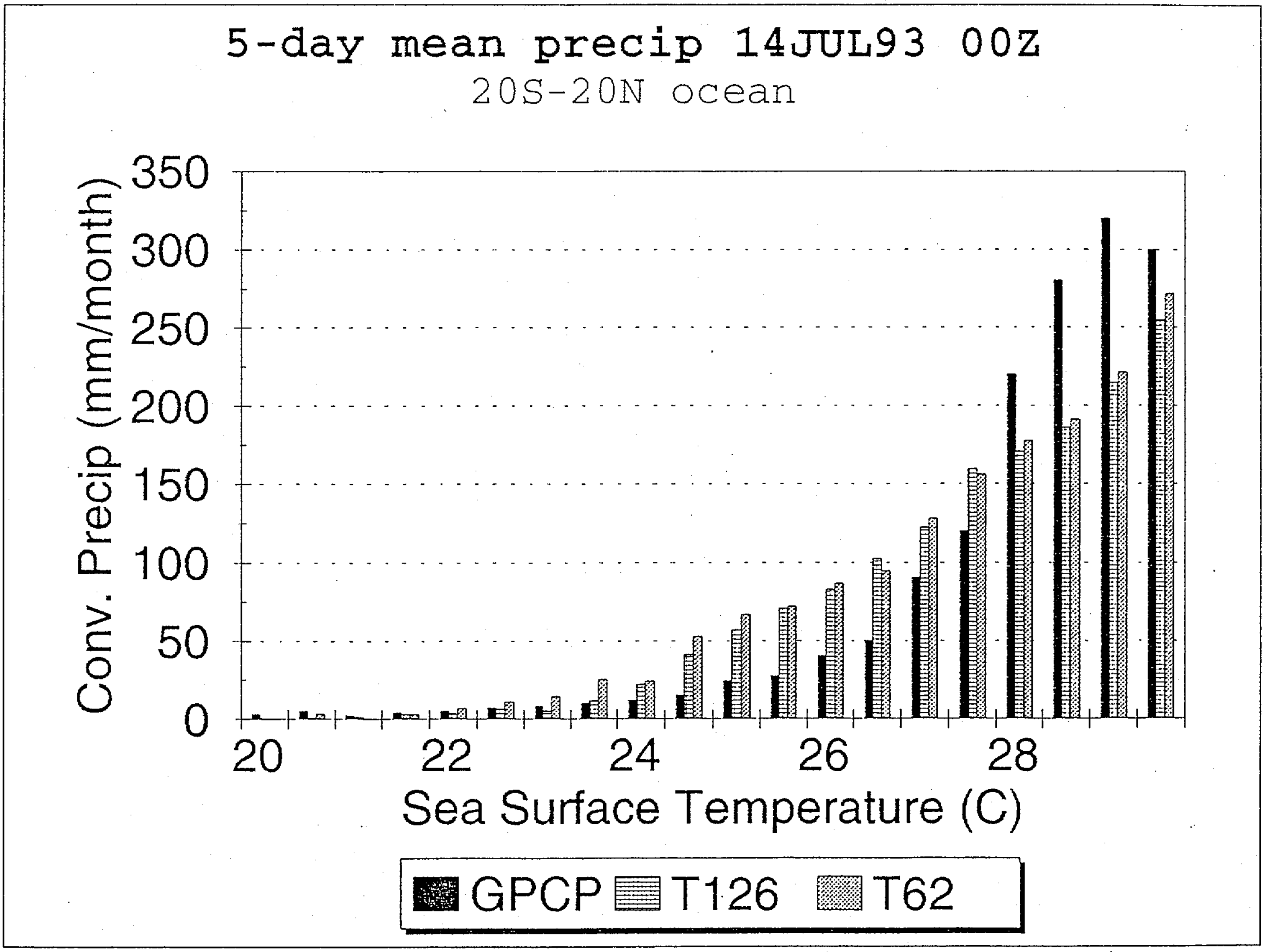

5-day mean precip 14JUL93 00Z
20S-20N ocean
Conv. Precip (mm/month)
0
50
100
150
200
250
300
350
20
22
24
26
28
Sea Surface Temperature (C)
GPCP
T126
T62

Fig. 14

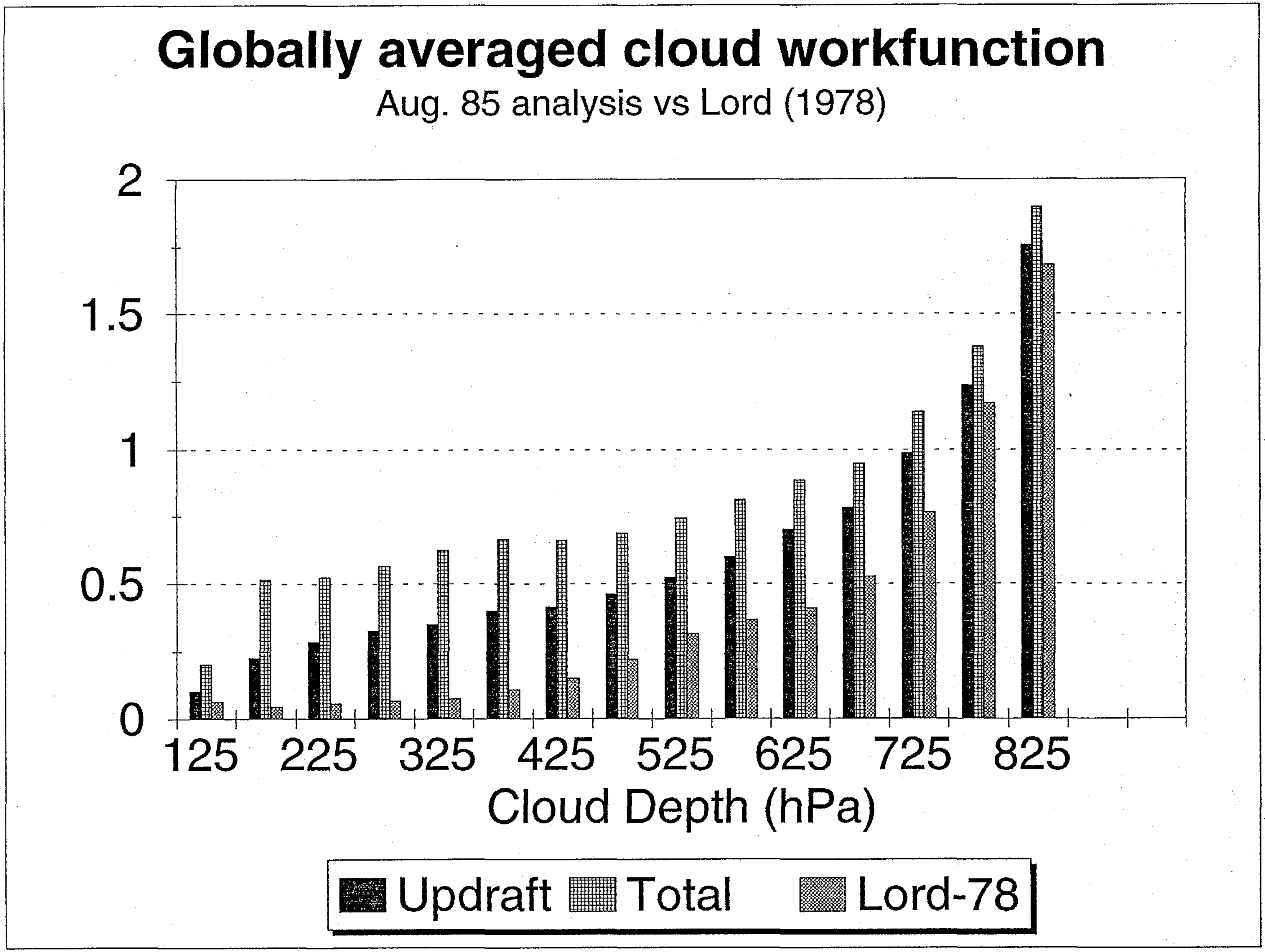

Globally averaged cloud workfunction
Aug. 85 analysis vs Lord (1978)
2
1.5
1
0.5
0
125
225
325
425
525
625
725
825
Cloud Depth (hPa)
Updraft
Total
Lord-78

Fig. 15

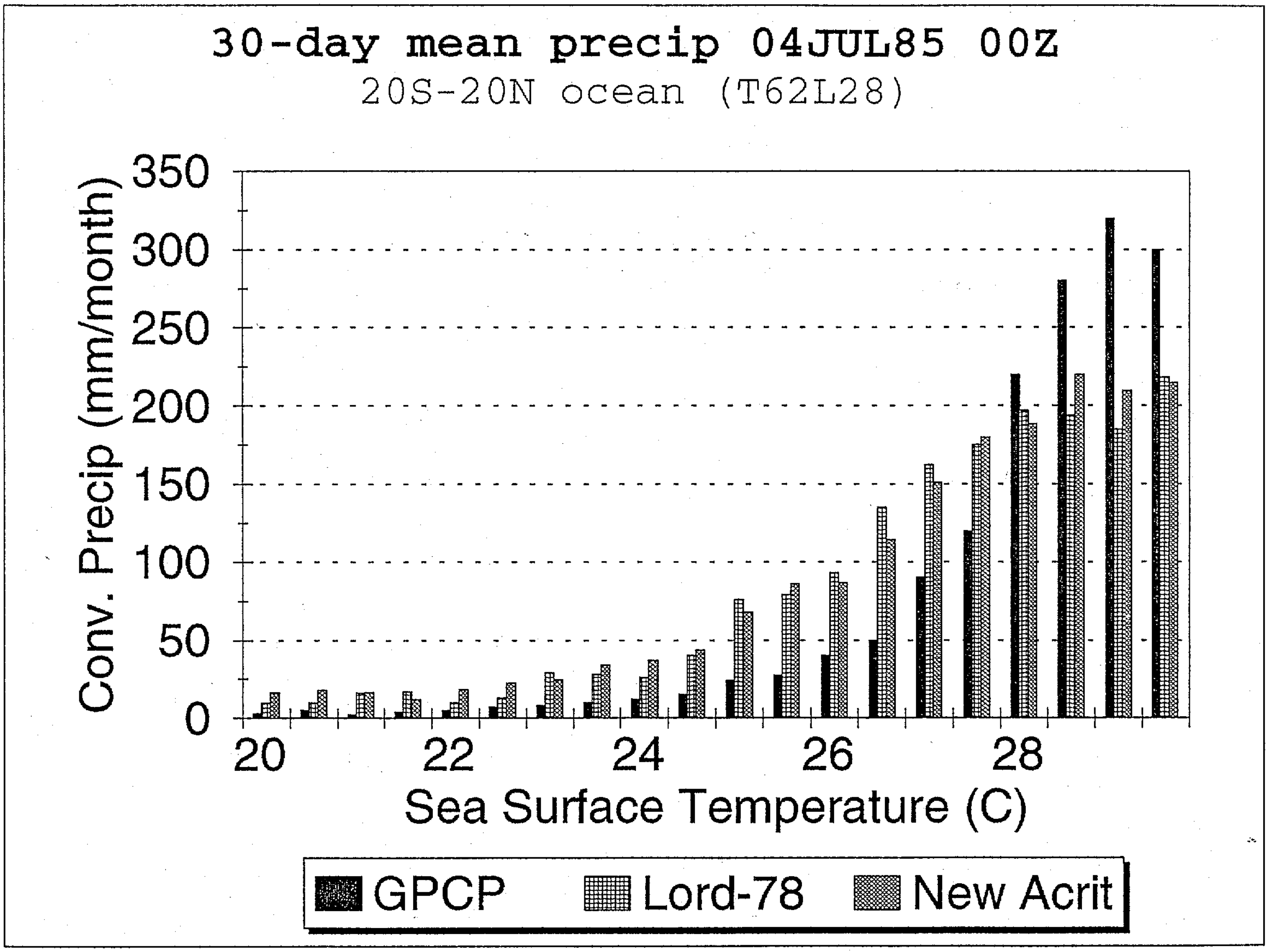
30-day mean precip 04JUL85 00Z
20S-20N ocean (T62L28)
Conv. Precip (mm/month)
350
300
250
200
150
100
50
0
20
22
24
26
28
Sea Surface Temperature (C)
GPCP
Lord-78
New Acrit

Fig. 16

hcnv day 16-31 average pilot 32 and 21

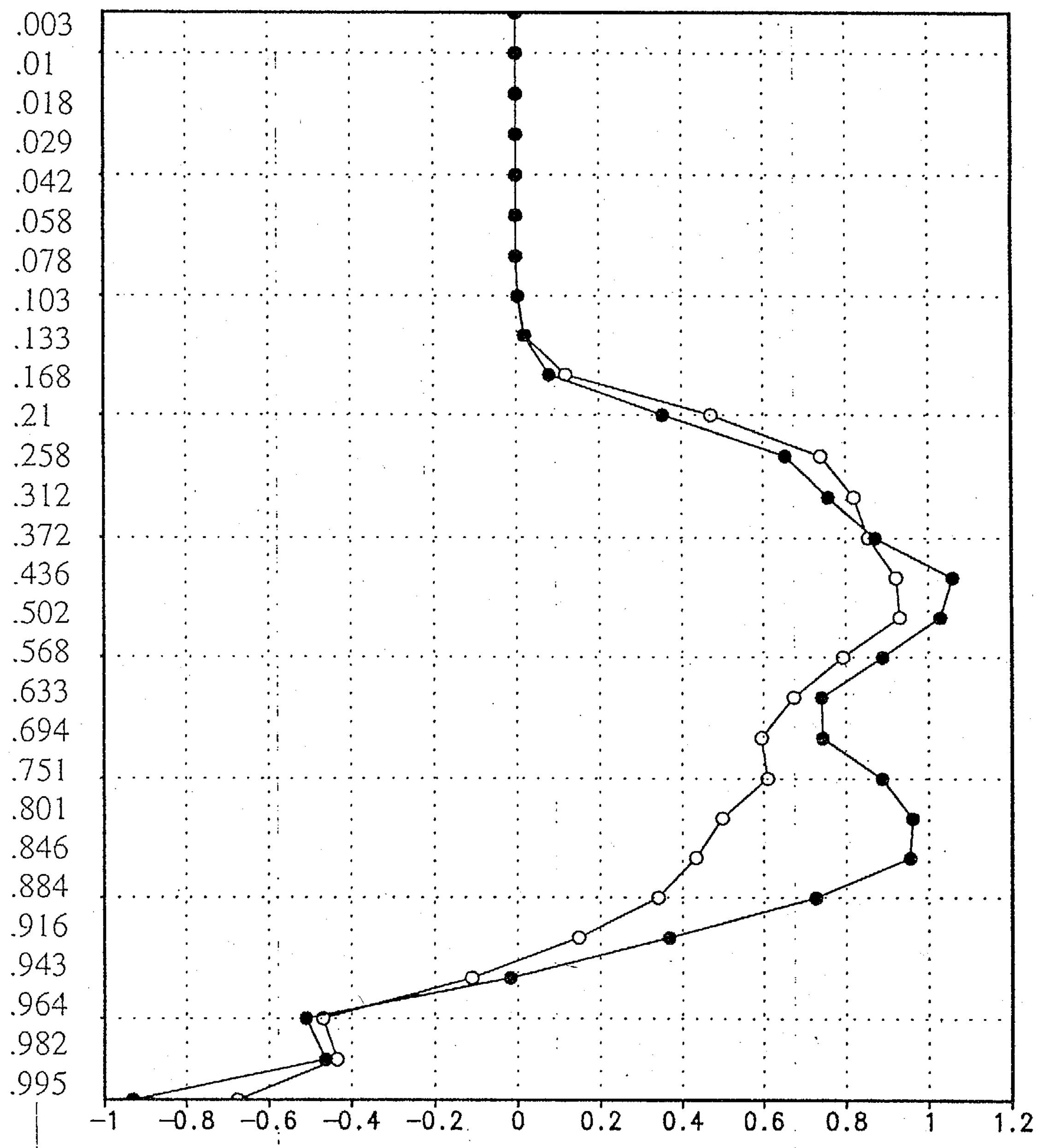

Fig.17

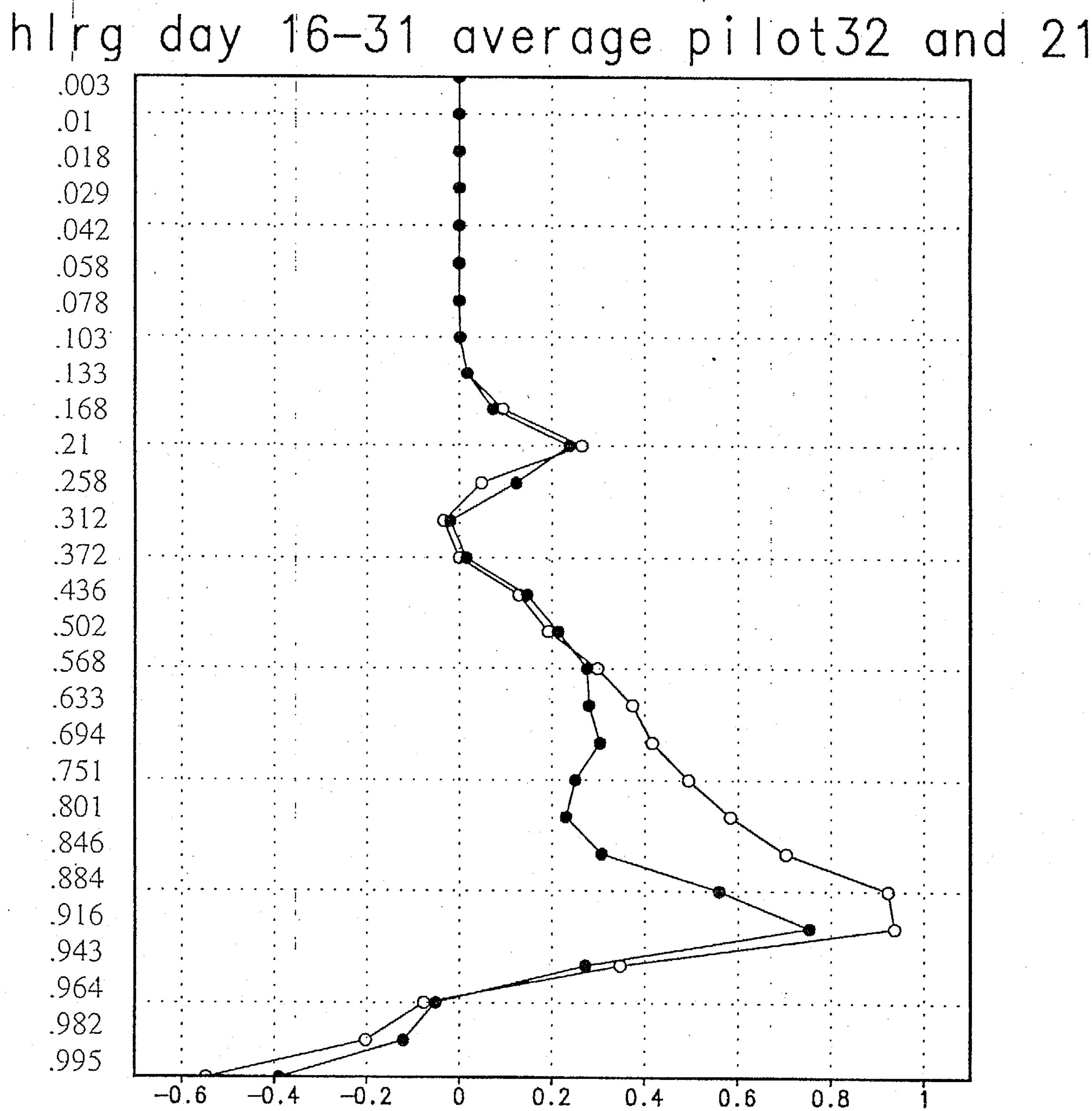

hlrg day 16–31 average pilot32 and 21
.003
.01
.018
.029
.042
.058
.078
.103
.133
.168
.21
.258
.312
.372
.436
.502
.568
.633
.694
.751
.801
.846
.884
.916
.943
.964
.982
.995
−0.6 −0.4 −0.2 0 0.2 0.4 0.6 0.8 1

Fig. 18

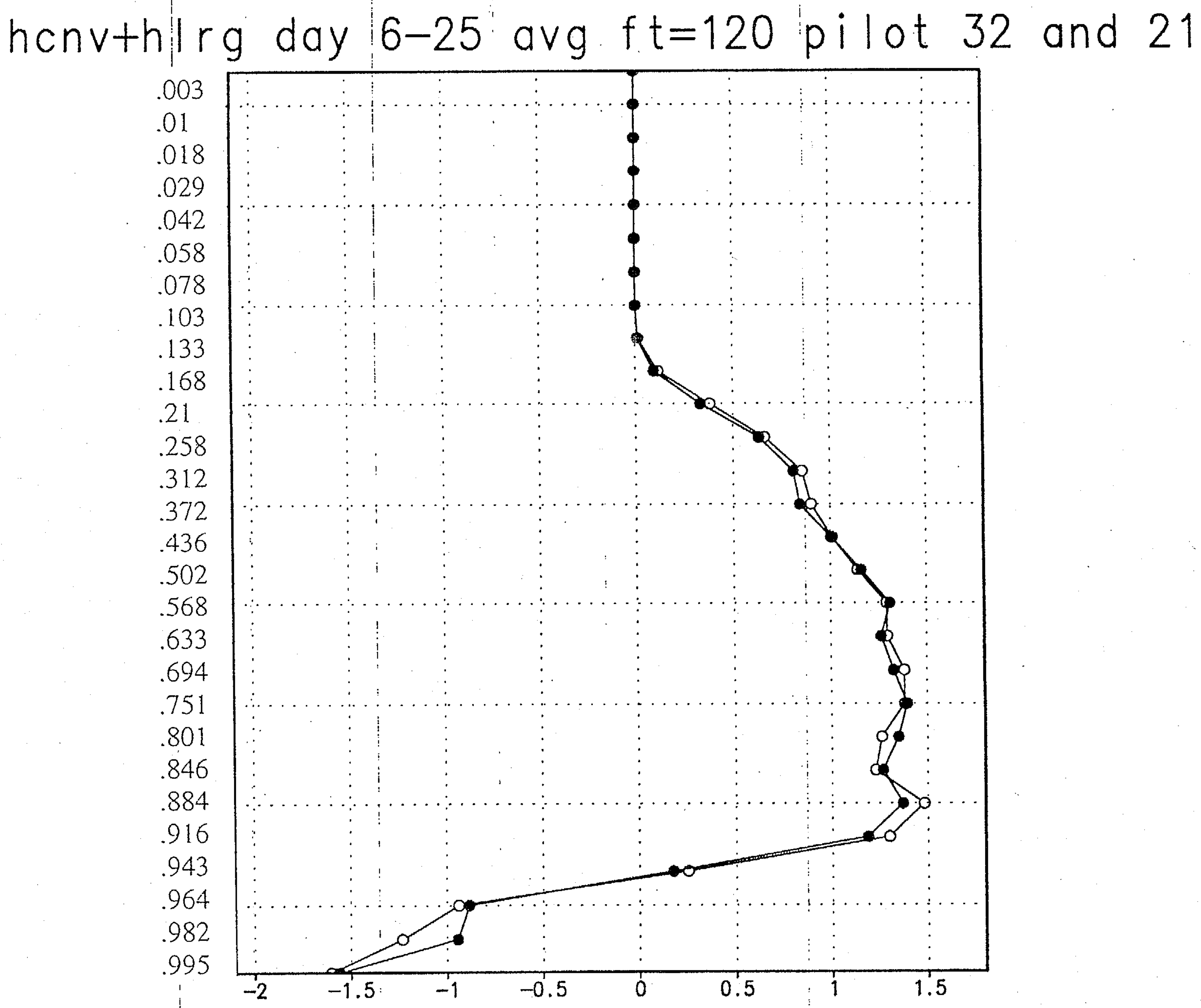

hcnv+hlrg day 6-25 avg ft=120 pilot 32 and 21
.003
.01
.018
.029
.042
.058
.078
.103
.133
.168
.21
.258
.312
.372
.436
.502
.568
.633
.694
.751
.801
.846
.884
.916
.943
.964
.982
.995
-2
-1.5
-1
-0.5
0
0.5
1
1.5

Fig. 19